

Microscopic scale simulation of the ablation of fibrous materials

Jean Lachaud* and Nagi N. Mansour†

NASA Ames Research Center, Moffett Field, CA, 94035, USA

Ablation by oxidation of carbon-fiber preforms impregnated in carbonized phenolic matrix is modeled at microscopic scale. Direct numerical simulations show that the carbonized phenolic matrix ablates in volume leaving the carbon fibers exposed. This is due to the fact that the reactivity of carbonized phenolic is higher than the reactivity of carbon fibers. After the matrix is depleted, the fibers ablate showing progressive reduction of their diameter. The overall material recession occurs when the fibers are consumed. Two materials with the same carbon-fiber preform, density and chemical composition, but with different matrix distributions are studied. These studies show that at moderate temperatures ($< 1000\text{ K}$) the microstructure of the material influences its recession rate; a fact that is not captured by current models that are based on chemical composition only. Surprisingly, the response of these impregnated-fiber materials is weakly dependent on the microstructure at very high temperatures (*e.g.*, Stardust peak heating conditions: 3360 K).

Nomenclature

C	Oxygen concentration, $\text{mol} \cdot \text{m}^{-3}$
D	Bulk diffusion coefficient, $\text{m}^2 \cdot \text{s}^{-1}$
J	Molar ablation rate, $\text{mol} \cdot \text{m}^{-2} \cdot \text{s}^{-1}$
k	Reactivity, $\text{m} \cdot \text{s}^{-1}$
Kn	Knudsen number
L	Characteristic length, m
\mathbf{n}	Vector normal to the surface
P	Pressure, Pa
\mathcal{R}	Ideal gas constant, $8.314\text{ J} \cdot \text{K}^{-1}$
s	Specific surface, $\text{m}^2 \cdot \text{m}^{-3}$
$S(x, y, z, t)$	Surface function
T	Temperature, K
\mathbf{v}	Velocity, $\text{m} \cdot \text{s}^{-1}$
Ω	solid molar volume, $\text{m}^3 \cdot \text{mol}^{-1}$
<i>Subscript</i>	
eff	Effective property
f	Fiber
g	Gas
i	Index
m	Matrix

*NASA Postdoctoral Program Fellow at NASA Ames Research Center, Reacting Flow Environments Branch, Mail Stop 230-3.

†Chief Division Scientist for Modeling and Simulation, Space Technology Division, Mail Stop 229-3, and AIAA Associate fellow.

Copyright © 2010 by the American Institute of Aeronautics and Astronautics, Inc. The U.S. Government has a royalty-free license to exercise all rights under the copyright claimed herein for Governmental purposes. All other rights are reserved by the copyright owner.

I. Introduction

A critical problem in the design of Thermal Protection Systems (TPS) for re-entry capsules is the choice of a heatshield material and its associated material response model. A new class of ablative materials has been introduced and validated in flight by the Stardust mission.¹ The use of this new class of low density Carbon/Resin (C/R) composites, made of a carbon fiber preform impregnated in phenolic resin, is being seriously considered for numerous forthcoming missions. PICA, the low density C/R developed at NASA Ames and used for Stardust, has been selected for Mars Science Laboratory (MSL) heatshield. PICA-X has been developed by SpaceX (Space Exploration Technologies Corp.) with the assistance of NASA to protect the Dragon capsule during re-entry ^a. The European Space Agency (ESA) is currently supporting the development of a light weight C/R ablator that could be used for sample return missions.²

The density of these materials lies around $300 \text{ kg} \cdot \text{m}^{-3}$. The carbon preform volume fraction is about 0.1. The density of carbon fibers typically ranges between 1600 and $2000 \text{ kg} \cdot \text{m}^{-3}$, depending on the fabrication process and the nature of the precursor. The carbon fiber preform accounts for about 60% of the mass, but occupies only 10% of the volume. The preform is impregnated in phenolic-formaldehyde resin in order to: (1) improve the mechanical properties of the virgin material, (2) benefit from the globally endothermic phenolic pyrolysis, (3) produce pyrolysis gases (blockage of the heat flux at the solid/fluid interface), (4) limit heat transport by radiation (significant above 800K), (5) prevent oxygen penetration in the porous preform (oxygen could oxidize the preform and deplete the structure's strength). The regular density of a dense phenolic-formaldehyde resin lies around $1200 \text{ kg} \cdot \text{m}^{-3}$. It is however possible using relevant impregnation techniques³ to produce an expanded structure with a lower apparent density. In order to reach the targeted material density ($300 \text{ kg} \cdot \text{m}^{-3}$), the porous carbon preform can be totally impregnated using an expanded pore-filling matrix of average density around $100 \text{ kg} \cdot \text{m}^{-3}$ (material B in Fig. 1) or partially impregnated using a dense fiber-coating matrix (material A Fig. 1). Any solution between these limit cases is of course conceivable.

Current ablation models would not distinguish material A from material B, because they have the same chemical composition and density. Inspired by the model of Kendall et al. published in 1968,⁴ current models describe ablation as a surface phenomenon occurring on a homogeneous, dense, and flat (no surface roughness) material.⁵⁻⁸ Equilibrium^{5,8} or finite-rate^{6,7} chemistry are considered in a control volume juxtaposed to the flat wall.⁴

The objective of the present work is to bring some insight to guide the development of volume ablation models based on a porous medium formalism (in contrast with a surface approach). We shall account for the facts that: (1) materials A and B have different structures; (2) their surface condition and/or porosity may evolve under ablative conditions; (3) an ablation zone may develop (instead of being confined to the surface). On the other hand, in order to start with a simple problem, we shall address the ablation by oxidation by molecular oxygen (under air) of the carbonized forms of materials A and B at constant temperature.

This work is divided in five sections. In the second section, we will present a general microscopic ablation model for heterogeneous materials. In the third section, we will describe the simulation tool used to solve this model at microscopic scale. In the fourth section, we will present, analyze, and compare the simulations of the ablation of material A and B in their carbonized form. In the fifth section, we will discuss the work hypotheses and how the presented approach could be used in the future. In the sixth section, we summarize the results and briefly describe future plans.

II. Microscopic ablation model for heterogeneous materials

Ablation is a non-mechanical physico-chemical process removing mater from a solid. The local motion of the material interface can be interpreted as a receding front with normal velocity proportional to the ablation rate.⁹ The interface is represented by a surface function $S(\mathbf{x},y,z,t)$ first order differentiable almost everywhere with constant value (zero) at the interface.¹⁰ The function S satisfies the differential equation

$$\partial_t S + \mathbf{v} \cdot \partial_{\mathbf{x}} S = 0 \quad (1)$$

where the recession velocity, \mathbf{v} , is modeled as

$$\mathbf{v} = \Omega J \mathbf{n} \quad (2)$$

^a<http://www.spacex.com/press.php?page=20090223>

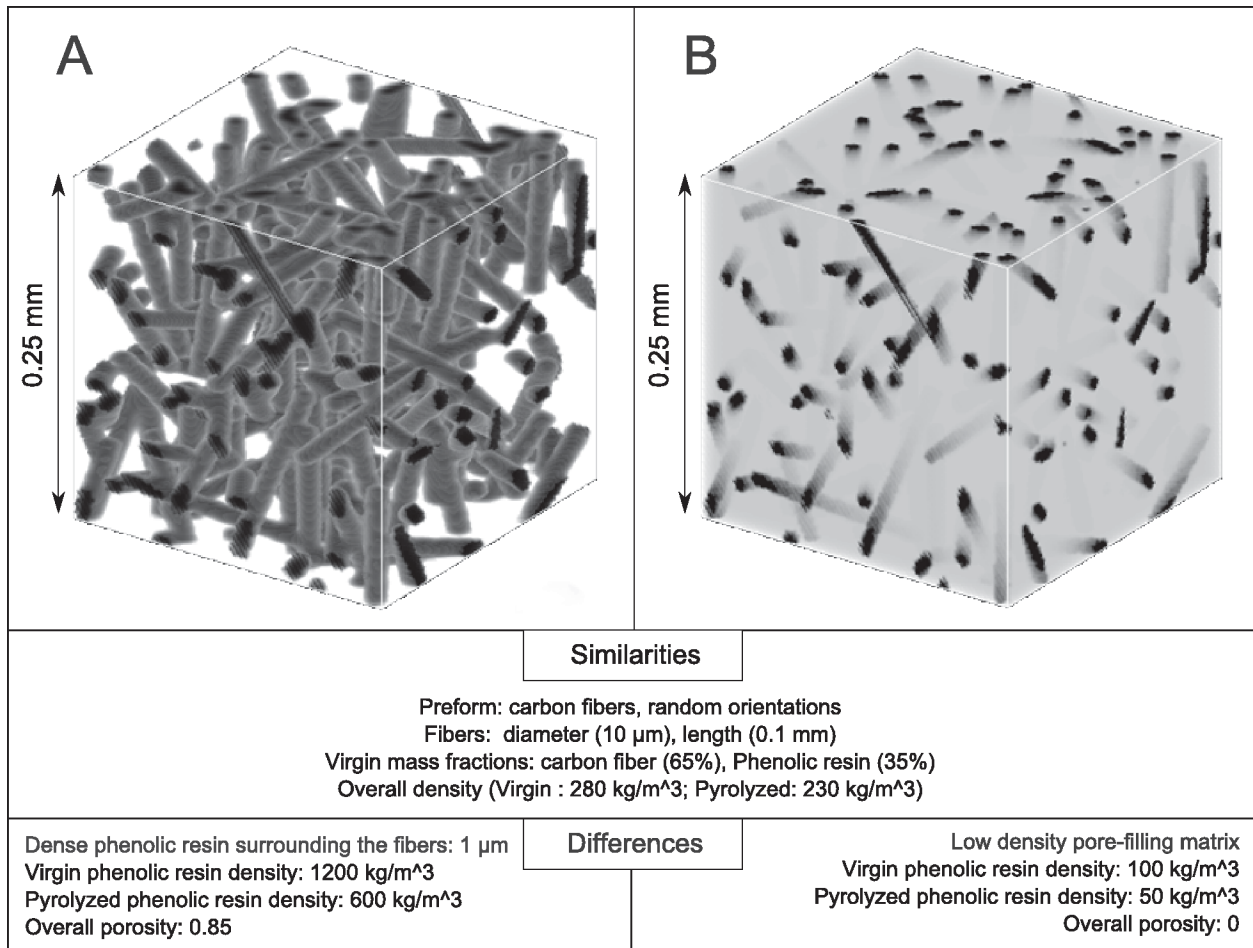


Figure 1. Two possible low density Carbon/Phenolic ablators with the same carbon-fiber preforms, density and chemical compositions, but with different matrix distributions.

with Ω the solid molar volume, J the ablation molar flux, and $\mathbf{n} = \partial_x S / \|\partial_x S\|$ the unit normal pointing outwards from the surface. In the case of the applications cited in the introduction, ablation may be due to oxidation and possibly sublimation. In the following, we shall consider ablation due to oxidation by molecular oxygen (under air), but a similar approach could be followed for oxidation by other species and for sublimation. We shall model carbon oxidation in air with a first order heterogeneous reaction.¹¹ For a first order heterogeneous reaction, the local impinging molar flux density (on a fiber or carbonized matrix elementary surface) is given by

$$J = k_i C \quad (3)$$

where $C = C(x, y, z, t)$ is the oxygen concentration and k_i is either the fiber, k_f , or the carbonized matrix, k_m , intrinsic reactivity. Fiber and carbonized matrix reactivities to molecular oxygen are estimated to lie around¹¹⁻¹⁴

$$k_f = \frac{k_m}{10} = 100 \exp\left(-\frac{1.2 \cdot 10^5}{RT}\right) \quad (4)$$

where T is the local temperature and \mathcal{R} the ideal gas constant. The reactivity of the matrix is higher than the reactivity of the fibers because the pseudo-graphitic structure of the carbonized phenolic matrix includes many more defects than carbon fibers.¹¹ The local concentration of oxygen is obtained by solving a mass balance equation featuring transport in the gas phase, from the wall and through the pores of the material if it is porous. The determination of the location of the average solid/surrounding fluid interface (wall) is not obvious for rough or porous media. In a first approximation, we will keep the current model hypothesis

and consider that the wall is defined by the surface delimited by the emerging fiber tips, as represented in Fig. 2.

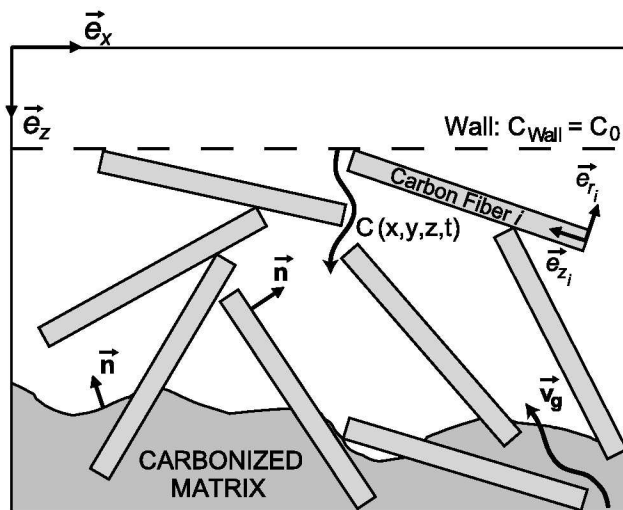


Figure 2. Sketch of the ablation the char layer of a Carbon/Resin material at microscopic (fiber) scale.

In the phase of the re-entry trajectory for which ablation is non-negligible, the flow dynamics are usually in the continuum regime at the scale of the re-entry body.¹⁵ However, inside the porous medium, the length-scale of interest is small and the dynamics may be in the rarefied gas regime. In porous media, the Knudsen number is defined as the ratio of the mean free path to the mean pore diameter. The mean pore diameter of the type of carbon preform that we are studying lies around $50 \mu m$. As a reference point, during the ablative part of the re-entry of Stardust, the mean free path for oxygen molecules reaches a minimum of $4 \mu m$ at peak heating. When ablation began, the Knudsen number in the porous medium was about 100; then, it has decreased to reach its minimal value of 0.08 at peak heating.¹⁴ Mass transport at the pore scale has to be modeled using different methods depending on the trajectory time. The Boltzmann equation is the fundamental mathematical model for gas flow at molecular scale.¹⁶ For dilute gas dynamics (rarefied and transitional regimes, *i.e.* $Kn > 0.1$), an efficient way to solve the Boltzmann equation is to follow a representative set of particles as they collide and move in physical space.¹⁷ This integration method is called Direct Simulation Monte Carlo (DSMC).¹⁶ A Monte Carlo simulation tool that models mass transfer in the porous medium using random walks is presented in the next section and used in section IV. For gas dynamics in the continuum regime ($Kn < 0.01$), the Navier-Stokes equations may be derived from the Boltzmann equation. This allows the use of analytical or CFD methods that are in general more efficient in the continuum regime than DSMC. In the slip regime ($0.02 < Kn < 0.1$), the continuum regime model may be used with allowing for discontinuities in velocity (slip) at solid boundaries.¹⁸

Using the continuum mechanics formulation of fluid dynamics, the local conservation of oxygen concentration in the fluid phase is given by

$$\partial_t C - \partial_{\mathbf{x}} \cdot (D \partial_{\mathbf{x}} C) + \partial_{\mathbf{x}} \cdot (C \mathbf{v}_{\mathbf{g}}) = 0 \quad (5)$$

where the second term models the binary diffusion of oxygen concentration in air according to Fick's law; D is the diffusion coefficient. The third term models the convective transport of oxygen concentration, where $\mathbf{v}_{\mathbf{g}}$ is the local velocity of the fluid. In re-entry applications, the fluid velocity is driven by the pressure gradients arising from the production of pyrolysis gases and by gas expansion due to temperature increase. We have shown in a previous study that the convective term is small compared to the diffusive term in flight conditions.¹⁴ In this study, we consider a carbonized material (already pyrolyzed) and an isothermal sample; hence, the fluid velocity is zero. When they are present, pyrolysis gases may react with the carbon preform (coking or oxidation) or with oxygen (homogeneous reactions). In this case, a source/sink term should be added in equation 5. For simple configurations, the system of equations 1-5 can be solved analytically in steady-state.^{9,14} In the case of random fibrous media and/or rarefied flows, direct numerical simulation (DNS) methods are required to find solutions on the micro-scale.

III. Simulation tool: AMA

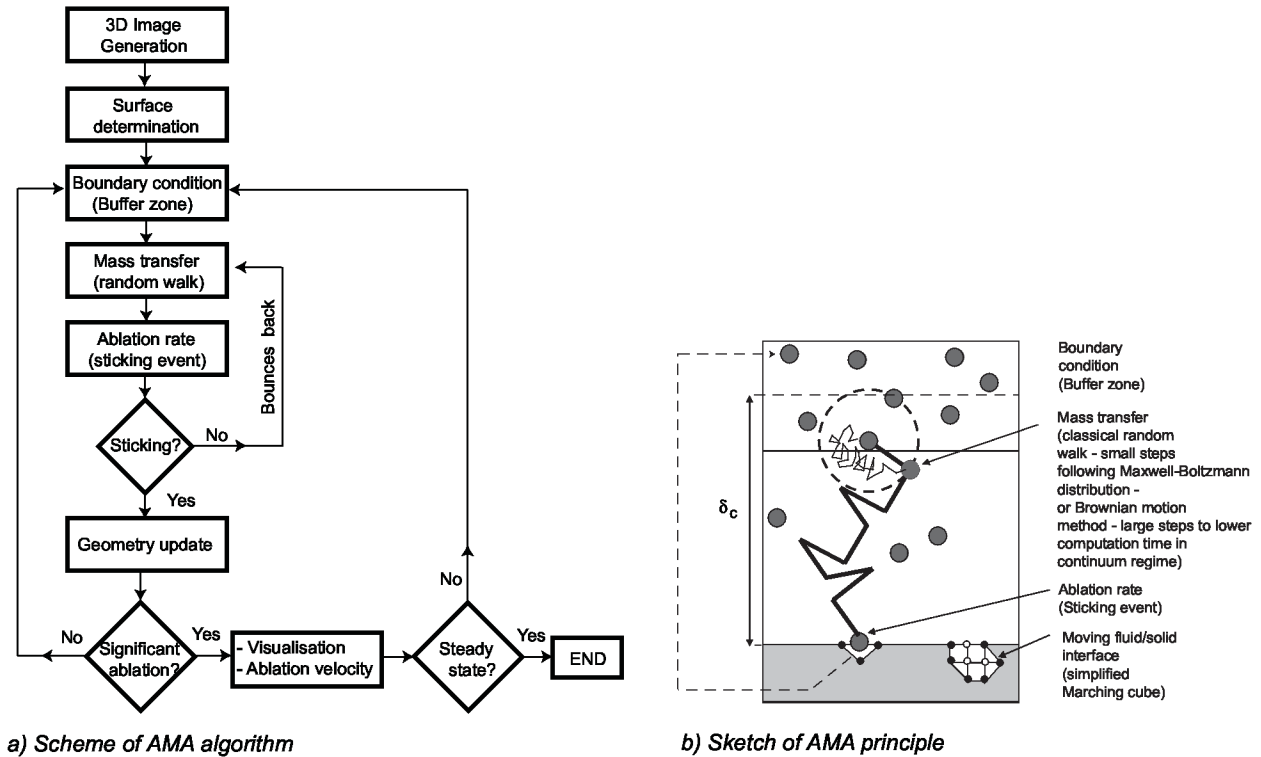


Figure 3. Description of AMA.

The 3-D time-dependent solution to the reaction/diffusion problem coupled to surface recession (described above) is obtained using a numerical simulation code, named AMA.¹⁹ The code uses Monte-Carlo random walk to simulate mass transfer from continuum to Knudsen regimes. A simplified description of AMA is presented in figure 3. AMA is a C ANSI implementation with four main features.

(a) A 3-D image (graph) containing several phases (fluid and solid in the present case) is described by the discrete cubic voxel method on a Cartesian grid. The size of the edges of the voxels is taken equal to $2.5\mu m$ in this study.

(b) The moving fluid/solid interfaces (Eq. 1) are determined by a simplified marching cube approximation.

(c) Mass transfer by diffusion (Eq. 5) is simulated by a random walk using Maxwell-Boltzmann distribution for the free path in the Knudsen and transition regimes, and a Brownian motion simulation technique in the continuum and slip regimes. Brownian motion is a grid-free method that efficiently converges when simulating diffusion in a continuous fluid.¹⁹

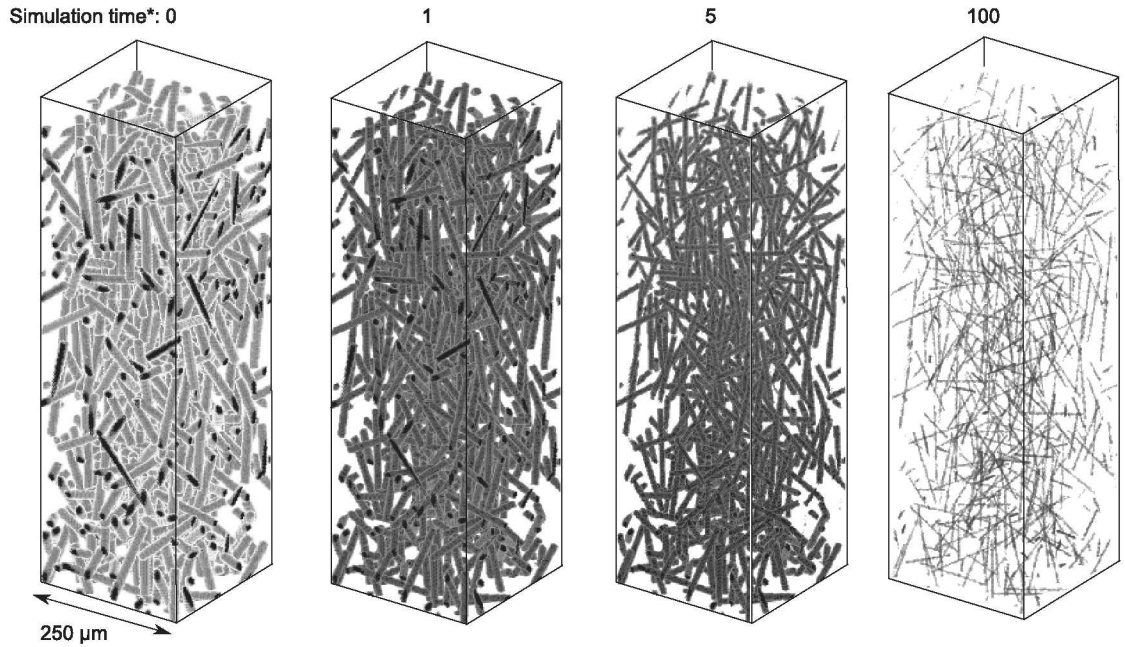
(d) Heterogeneous first-order reaction on the wall (Eq. 3) is simulated by using a sticking probability approach.

The boundary conditions are: Dirichlet on top of the domain, i.e. the oxygen concentration is specified, $C = C_0$, Neumann at the bottom (no oxygen flux), and periodic on the sides. Dirichlet boundary condition is handled using a buffer region where the concentration of walkers is kept constant.

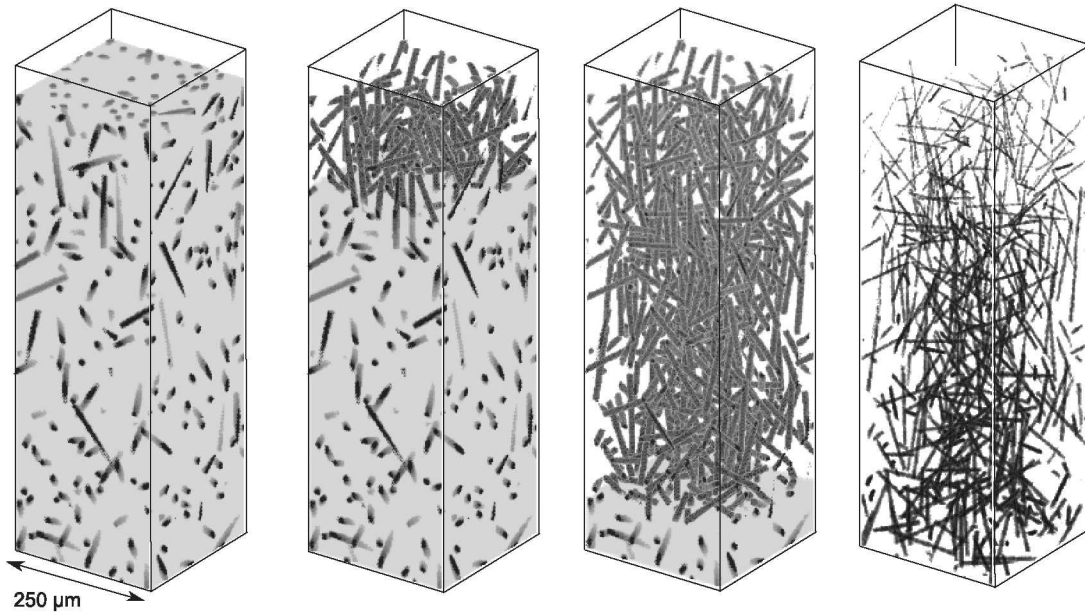
IV. Simulation of the ablation of materials A and B

We wish to understand and compare the ablative behaviors of materials A and B in their charred form (the phenolic resin is carbonized and no pyrolysis gas is produced). We shall consider ablation by oxidation under air at a constant temperature (no temperature gradient). The simulation are done using AMA on a cell of dimensions ($x = 0.25\text{ mm}$, $y = 0.25\text{ mm}$, $z = 0.75\text{ mm}$) containing 716 fibers. The cell is periodic in x and y directions. We are presenting simulation results for two sets of conditions identified by their Thiele number. In a previous study,¹⁴ we have shown the effect of the Thiele number on the ablative behavior of a

Small Thiele number ($\Phi < 0.05$), moderate temperature ($T < 1000K$)



a) Material A : C/R with carbonized fiber-coating matrix



b) Material B : C/R with carbonized pore-filling matrix

Similarities

- 1) At $t=0$, the matrix covers the fibers
- 2) The matrix, which is more reactive and less dense than the fibers, is ablated first
- 3) When the matrix is removed, the fibers themselves are ablated through a progressive reduction of their diameter
- 4) Once the matrix is ablated, A and B display the same behavior
- 4) The fiber preform vanishes in volume
- 5) No ablation front is observed

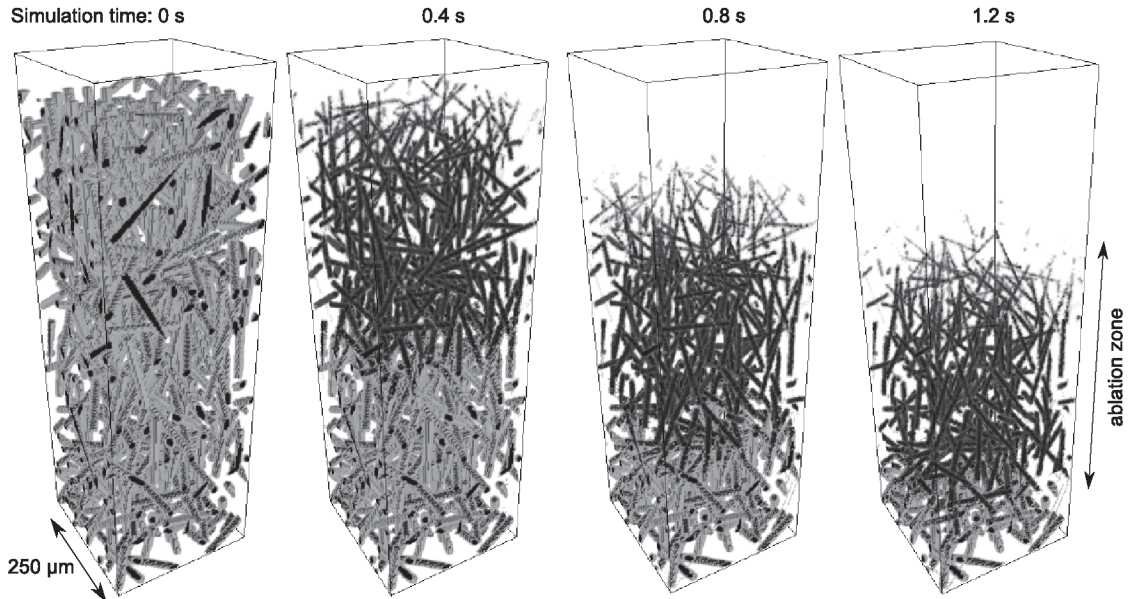
Differences

- 1) At $t=0$, oxygen diffusion in material A is possible (not in material B)
- 2) In material B, the matrix is progressively ablated featuring a recession front for the matrix
- 3) In material A, no recession front is observed for the matrix; the matrix is homogeneously ablated in depth

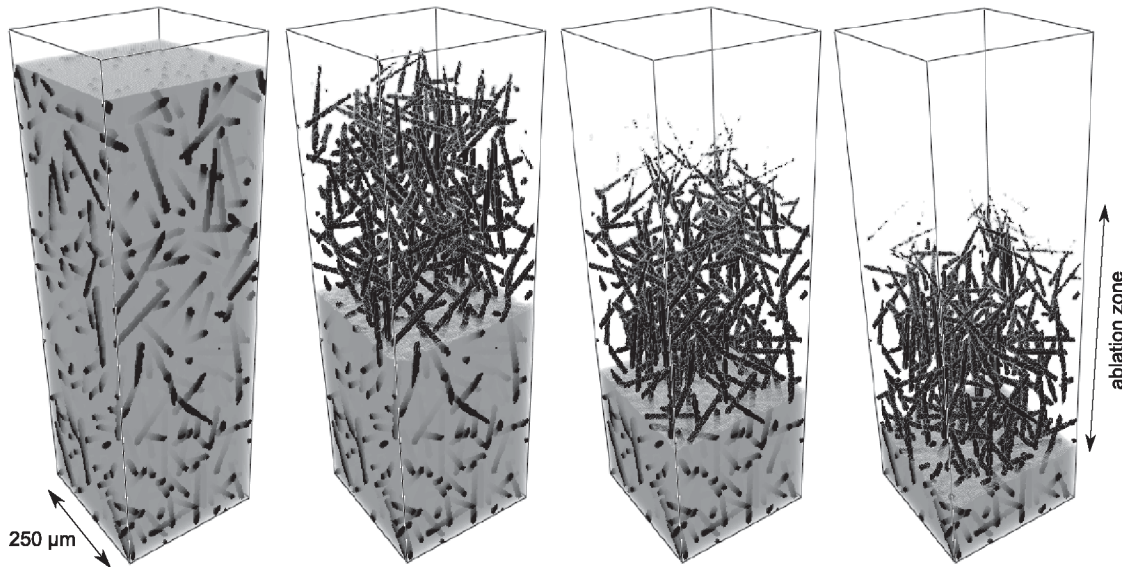
c) Comparison of the ablative behaviors of A and B in their charred state (similarities versus differences)

Figure 4. Comparison of the ablation response of a carbon preform with carbonized fiber-coating matrix (material A) and with carbonized pore-filling matrix (material B). Conditions: Isotherm ($T < 1000 K$), isobaric ($P = 0.26 atm$), under air. *Simulation time normalized to the time necessary to ablate the matrix layer, which depends on the chosen conditions. At 1000 K, the value of the time unit is 4 minutes.

Moderate Thiele number ($\Phi=4$), high temperature ($T=3600K$)



a) Material A : C/R with carbonized fiber-coating matrix



b) Material B : C/R with carbonized pore-filling matrix

Similarities

- 1) At $t=0$, the matrix covers the fibers
- 2) The matrix, which is more reactive and less dense than the fibers, is ablated first
- 3) When the matrix is removed, the fibers themselves are ablated through a progressive reduction of their diameter
- 4) When the top fibers are totally ablated (i.e., their diameter tends to zero), we observe an overall material recession
- 5) After an initialization period, in both cases oxygen has to diffuse through the fibrous preform to oxidize the matrix
- 6) The carbon preform protects the matrix by consuming a part of the oxygen and slowing the diffusion process
- 7) We can distinguish two recession fronts: the first one is delimited by the tip of the fibers (fiber front); the second one is the matrix front. The material density decreases from the matrix front to the fiber front. We propose to call the layer of material lying between these two fronts, the ablation zone.
- 8) In both cases, the depth of the ablation zone increases during a transient regime until it reaches a constant value, leading to a permanent regime.

Differences

- 0) None, but for different reasons :
 - in material A, oxygen cannot penetrate in the fibrous medium if there is some matrix available because all the oxygen is consumed by the very reactive matrix
 - in material B, the pore-filling matrix forms a natural barrier to oxygen diffusion

c) Comparison of the ablative behaviors of A and B in their charred state (similarities versus differences)

Figure 5. Comparison of the ablation response of a carbon preform with carbonized fiber-coating matrix (material A) and with carbonized pore-filling matrix (material B). Conditions: Isotherm ($T = 3360 K$), isobaric ($P = 0.26 atm$), under air.

carbon preform. For a fibrous preform (without matrix), the Thiele number is defined as

$$\Phi = \frac{L}{\sqrt{D_{eff}/(s_f k_f)}} \quad (6)$$

where L is the characteristic length of interest (*e.g.* the depth of the considered cell), D_{eff} the effective diffusion coefficient, s_f the fiber specific surface, and k_f the fiber reactivity. When the reaction rate is fast compared to the mass-transfer rate (high Thiele number), the oxidant is mostly consumed at the surface and cannot diffuse through the fibrous preform; in this case, ablation is a surface process, *i.e.* the thickness of the ablation zone is not large compared to fiber diameter. In the converse case (moderate to low Thiele number), the oxidant consumption rate being slow compared to the mass-transfer rate, the oxidant concentration becomes homogeneous inside the fibrous preform and ablation occurs in volume. In the frame of our study, the case of high Thiele numbers is trivial. Matrix and fibers would recess at the same velocity leading to a uniform recession of the material, often called *surface ablation*. In the case of the ablative applications mentioned in the introduction, the diffusion coefficient is large when ablation occurs because the density of the gas is small. Therefore, high Thiele numbers are not encountered in these applications. In this study, we shall simulate ablation at low and moderate Thiele numbers:

1) In figure 4, we are presenting the simulation results of the ablation of materials A and B at low Thiele number ($\Phi < 0.05$). [To enable a comparison with the next case, these conditions are attained for temperatures lower than 1000 K at a pressure of 0.26 atm .]

2) In figure 5, we are presenting the simulation results of the ablation of materials A and B at a moderate Thiele number ($\Phi = 4$). We have chosen Stardust peak-heating temperature (3360 K) and pressure (0.26 atm) at the stagnation point.¹⁵

In both conditions, the recession is faster for the matrix than for the fibers. This is explained by the fact that (1) the reactivity of the carbonized matrix is ten times higher than the reactivity of the fibers, and (2) the matrix to fiber density ratio is around 2:3 for material A and 1:32 for material B.

In the case of material B, progressively, the matrix is ablated and the fibers are stripped out and oxidized leading to their thinning (figures 4-b and 5-b). When a steady state is reached (last pictures of the series), we can distinguish two recession fronts: the first front is delimited by the tip of the fibers (fiber front); the second front is the matrix front. The material density decreases from the matrix front to the fiber front. We propose to call the layer of material lying between these two fronts, the *ablation zone* (depicted in figure 5).

At moderate Thiele number, material A displays a behavior similar to the behavior of material B (figure 5-a). This is explained by the fact that the carbonized matrix is very reactive at high temperature. The Thiele number evaluated for the matrix reactivity would be 40. Therefore, the matrix has a high Thiele number behavior; *i.e.*, it consumes all the oxygen available at its effective surface. The oxygen cannot penetrate deeper than the matrix front inside the porous medium. For this reason, the steady-state ablation zone has the same size at moderate Thiele number for both materials (last images of figures 5-a and b). At small Thiele number, material A behaves differently than material B. In this case, oxygen can penetrate inside the pores of the carbonized material. The carbonized matrix coat is ablated at the same time at all levels; then the fibers are ablated and the whole structure progressively vanishes.

V. Discussion

At moderate temperatures, current models overestimate ablation rates because equilibrium chemistry is an upper-bound model (compared to possible finite-rate chemistry). Stardust post-flight analyses have shown that the recessions on the flank and near the stagnation point are respectively overestimated by 20% and 61% using this description.¹ Finite-rate chemistry models have been proposed, implemented, tested, and shown to improve the accuracy of current models.^{6,7} However, in these studies, the surface of the material is still considered flat and homogeneous. Accurate finite-rate heterogeneous chemistry models would require an estimate of the effective reactive surface area (ERSA) of the wall material. This is a complicated problem because the ERSA evolves with time and conditions as shown in this study. In the case of porous materials, the ERSA is a complex function of the porosity of the material and of the mass transport inside the pores. Recently, a model predicting the ERSA of fibrous preforms has been proposed.¹⁴ It has been found that for typical re-entry conditions the effective reactivity of the fibrous preform could be two order of magnitude as large as the intrinsic reactivity of the individual fibers. The same kind of discrepancy is expected when modeling ablative materials if the accessible surface increase due to volume ablation is not negligible and

not accounted for. To extend the present model to ablative materials and re-entry conditions, it would be necessary to complete the chemistry model and to account for temperature gradients.

VI. Conclusion

A new microscopic approach to study the ablation by oxidation of carbonized low-density C/R has been proposed. The details of the architecture of the materials are modeled (fiber size, position and orientation, and matrix repartition). A layer of 0.75 mm of fibrous material, containing 716 fibers, is considered. The surface recessions of the matrix and of each fiber are tracked as they are ablate. Local (microscopic) surface recession and oxygen consumption are coupled to mass transfer in the porous medium. Two materials with the same carbon-fiber preform, density and chemical composition, but with different matrix distributions are studied. One has a pore-filling matrix, the other one has a fiber-coating matrix. Direct numerical simulations show that in both cases, the matrices are ablated in volume leaving the carbon fibers unprotected. This is due to the fact that the reactivity of carbonized phenolic is higher than the reactivity of carbon-fibers. When the matrix is removed, the fibers themselves are ablated through a progressive reduction of their diameter. The overall material recession occurs when the fibers are consumed. The materials are shown to behave differently in the transient regime at low Thiele numbers (e.g., air, $T = 1000\text{ K}$, $P = 0.26\text{ atm}$). The pore-filling matrix provides better ablative protection to the carbon-fiber preform than the fiber-coating matrix. Paradoxically, both materials display similar behaviors at moderate and large Thiele numbers (e.g., air, $T = 3360\text{ K}$, $P = 0.26\text{ atm}$). The Thiele number is an estimator of the reaction/diffusion competition for porous media. It increases with the reactivity and decreases with the diffusion coefficient. The presented microscopic model points out two trends regarding the ablative behavior of fibrous materials:

- The microscopic architecture is a parameter that may affect the ablative response of a material. (Chemical composition and density are two other well know parameters.)
- Ablation may occur in volume. The introduction of an ablation zone in current models may help in improving their accuracy.

In the future, we would like to extend the model to raw ablative materials (including pyrolysis and reaction of oxygen with pyrolysis gases) and to re-entry conditions (including thermal gradients and sublimation).

Acknowledgments

This research was supported by the fundamental aeronautics program - hypersonics project. JL would like to acknowledge appointment to the NASA Postdoctoral Program at the Ames Research Center, administered by Oak Ridge Associated Universities.

References

- ¹Stackpoole, M., Sepka, S., Cozmuta, I., and Kontinos, D., "Post-Flight Evaluation of Stardust Sample Return Capsule Forebody Heatshield Material," AIAA paper 2008-1202, Jan. 2008.
- ²Ritter, H., Portela, P., Keller, K., Bouilly, J. M., and Burnage, S., "Development of a European Ablative Material for Heatshields of Sample Return Missions," 6th European Workshop on TPS and Hot structures, Stuttgart, Germany, 1-3 April 2009.
- ³Tran, H. K., Johnson, C. E., Rasky, D. J., Hui, F. C. L., Hsu, M.-T., Chen, T., Chen, Y. K., Paragas, D., and Kobayashi, L., "Phenolic Impregnated Carbon Ablators (PICA) as Thermal Protection Systems for Discovery Missions," NASA Technical Memorandum 110440, 1997.
- ⁴Kendall, R. M., Bartlett, E. P., Rindal, R. A., and Moyer, C. B., "An Analysis of the Coupled Chemically Reacting Boundary Layer and Charring Ablator: Part I," NASA CR 1060, 1968.
- ⁵Milos, F. and Chen, Y.-K., "Ablation and Thermal Response Property Model Validation for Phenolic Impregnated Carbon Ablator," AIAA paper 2009-262, Jan. 2009.
- ⁶Chen, Y.-K. and Milos, F., "Navier-Stokes Solutions with Finite Rate Ablation for Planetary Mission Earth Reentries," *Journal of Spacecraft and Rockets*, Vol. 42, No. 6, 2005, pp. 961-970. doi: 10.2514/1.12248.
- ⁷Beerman, A., Lewis, M., Starkey, R., and Cybyk, B., "Non-equilibrium Surface Interactions Ablation Modeling with the Fully Implicit Ablation and Thermal Response Program," AIAA paper 2008-1224, Jan. 2008.
- ⁸Martin, A. and Boyd, I. D., "Implicit Implementation of Material Response and Moving Meshes for Hypersonic Re-Entry Ablation," AIAA paper 2009-670, Jan. 2009.

⁹Lachaud, J., Aspa, Y., and Vignoles, G. L., "Analytical Modeling of the Steady State Ablation of a 3D C/C Composite," *International Journal of Heat and Mass Transfer*, Vol. 51, No. 9–10, 2008, pp. 2614–2627. doi:10.1016/j.ijheatmasstransfer.2008.01.008

¹⁰Katardjiev, I. V., Carter, G., Nobes, M. J., Berg, S., and Blom, H.-O., "Three-Dimensional Simulation of Surface Evolution during Growth and Erosion," *Journal of Vacuum Science and Technology A*, Vol. 12, No. 1, 1994, pp. 61–68.

¹¹Lachaud, J., Bertrand, N., Vignoles, G. L., Bourget, G., Rebillat, F., and Weisbecker, P., "A Theoretical/Experimental Approach to the Intrinsic Oxidation Reactivities of C/C Composites and of their Components," *Carbon*, Vol. 45, No. 14, 2007, pp. 2768–2776. doi:10.1016/j.carbon.2007.09.034.

¹²Park, C., "Nonequilibrium Hypersonic Aerothermodynamics," John Wiley & Sons, New York, 1990.

¹³Drawin, S., Bacos, M. P., Dorvaux, J. M., and Lavigne, O., "Oxidation Model for Carbon-Carbon Composites," AIAA paper 92-210, Jan. 1992.

¹⁴Lachaud, J., Cozmuta, I., and Mansour, N. N., "Multiscale Approach to Ablation Modeling of Phenolic Impregnated Carbon Ablators," *Journal of Spacecraft and Rockets*, in press.

¹⁵Trumble, K. A., Cozmuta, I., Sepka, S., and Jenniskens, P., "Post-flight Aerothermal Analysis of the Stardust Sample Return Capsule," AIAA paper 2008-1201, Jan. 2008.

¹⁶Bird, G. A., *Molecular Gas Dynamics and the Direct Simulation of Gas Flow*, Oxford science publication, Oxford, Great Britain, 1994.

¹⁷Boyd, I., "Direct Simulation Monte Carlo for Atmospheric Entry," *Course on hypersonic entry and cruise vehicles*, edited by O. Chazot, VKI LS, Rhode-Saint-Genese, Belgium, 2008.

¹⁸Anderson, J. D., *Hypersonic and High Temperature Gas Dynamics*, Mac Graw-Hill, New-York, 1989.

¹⁹Lachaud, J. and Vignoles, G. L., "A Brownian Motion Technique to Simulate Gasification and its Application to C/C Composite Ablation," *Computational Material Science*, Vol. 44, No. 4, 2008, pp. 1034–1041. doi:10.1016/j.commatsci.2008.07.015



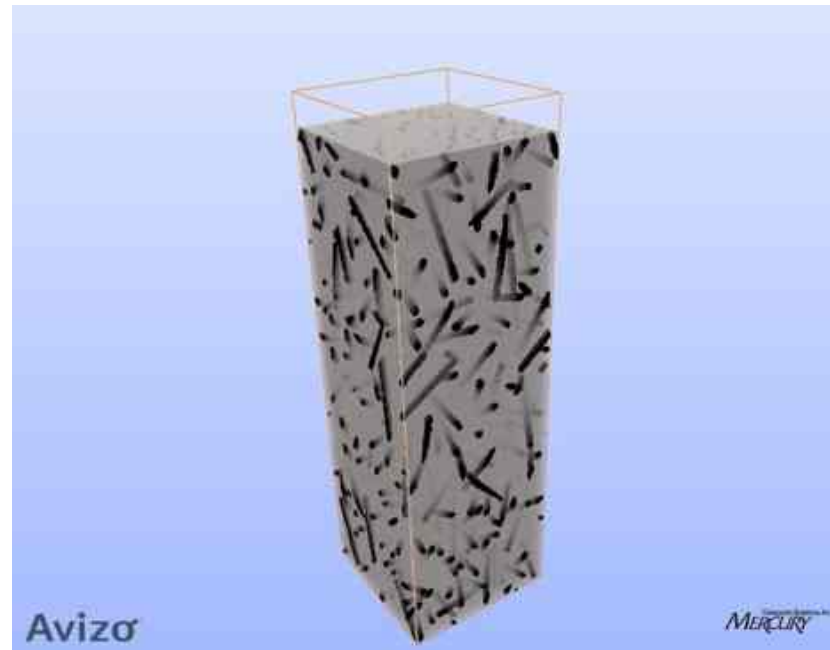
Microscopic scale simulation of the ablation of fibrous materials

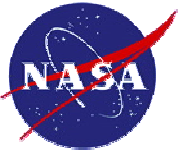
Jean Lachaud* and Nagi N. Mansour⁺

* NASA Postdoctoral Program Fellow at NASA Ames, Jean.R.Lachaud@nasa.gov

Sponsored by NASA's Fundamental Aeronautics Program - Hypersonics Project

⁺ NASA Ames Research Center, Nagi.N.Mansour@nasa.gov



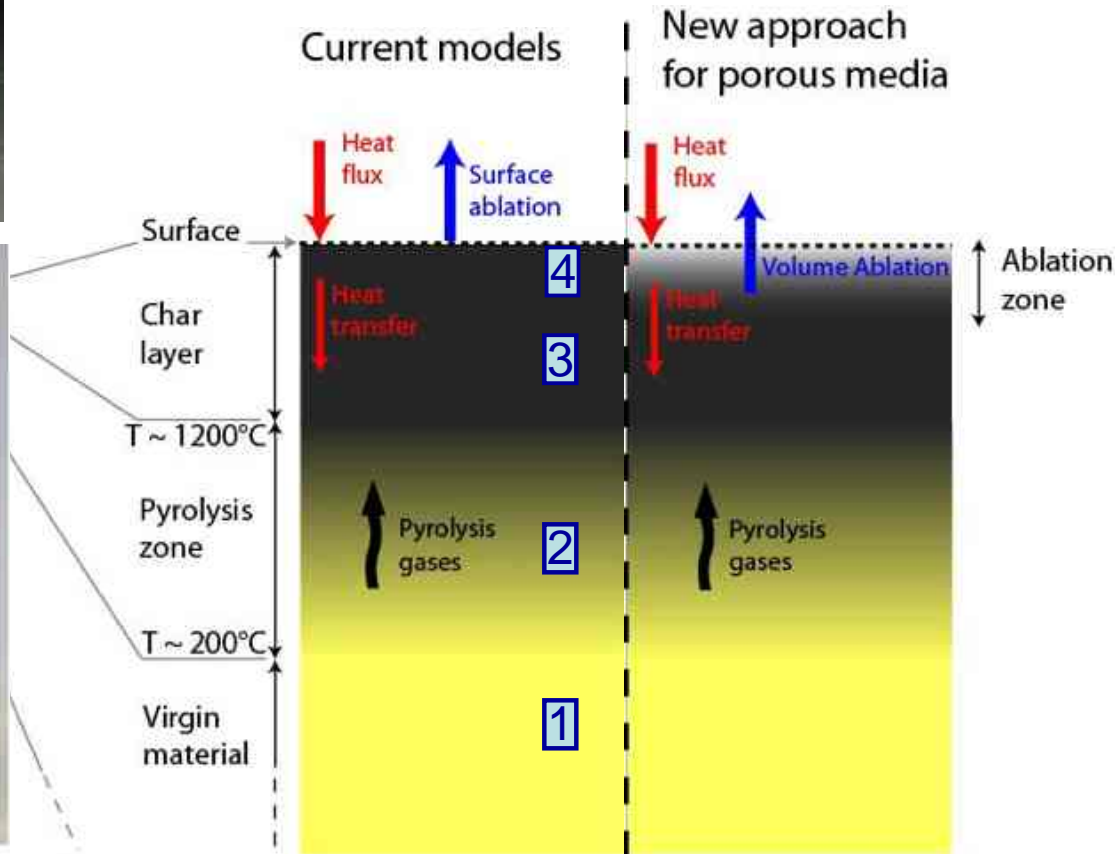


. Introduction : (a) observation

Fibrous Thermal Protection Systems (TPS); e.g. Stardust and PICA



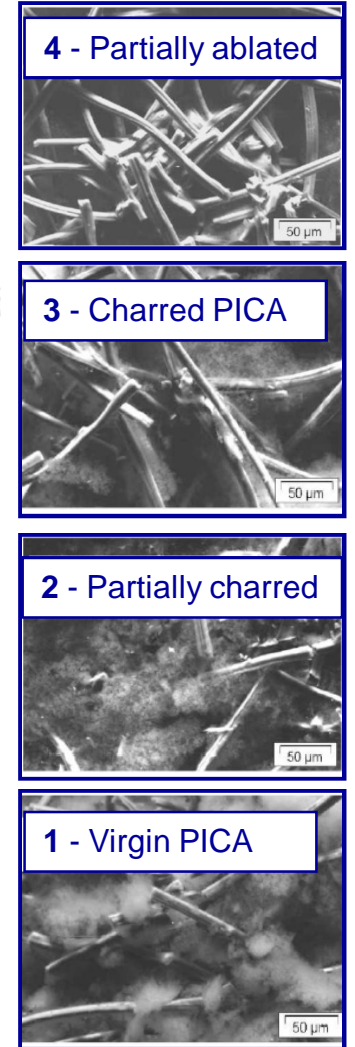
Core - Stardust TPS⁽¹⁾



First step for the porous medium approach : oxidation

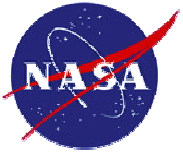
SEM 3 and 4 suggest the occurrence of some volume phenomena in the char layer:

- Oxidation (oxygen from the atmosphere)
- Sublimation
- Mechanical erosion of the matrix



SEM micrographs⁽¹⁾

[1] M. Stackpoole *et al.*, Post-Flight Evaluation of Stardust Sample Return Capsule Forebody Heatshield Material, AIAA 2008-1202



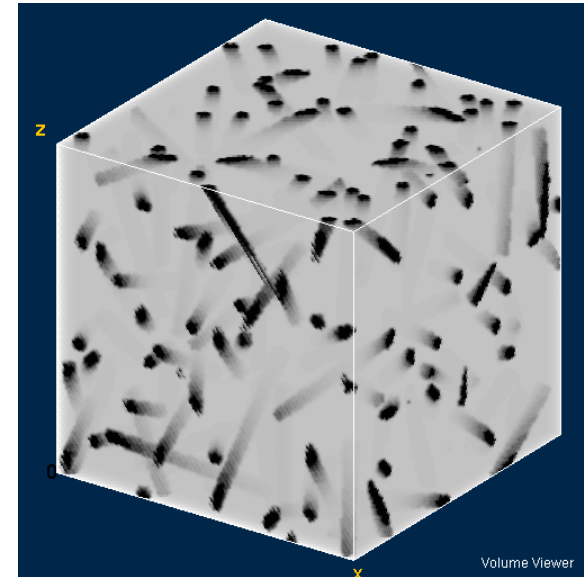
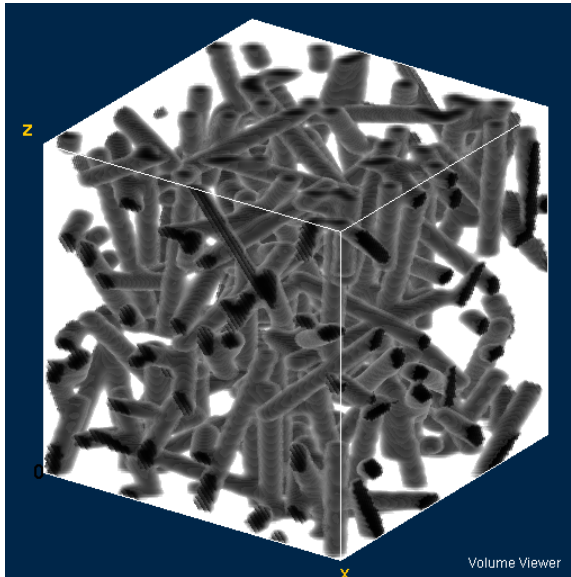
. Introduction : (b) comparison of 2 materials

Equilibrium chemistry vs. Finite-rate chemistry

Same fibrous preform, chemical composition, overall density

A : dense matrix layer around the fibers

B : Expanded, low density pore-filling matrix



- “Surface ablation” model (as described by *Kendall et al.*, NASA CR-1060, 1968)
 - Equilibrium chemistry → Only the chemical composition is important
 - model for A = model for B (in a control volume above the effective surface)
- “Ablation-zone model” model
 - Finite-rate chemistry → Material architecture is also important
 - model for A ≠ model for B (surface roughness and porosity are modeled)



. Outline

Microscopic scale simulation of the ablation of fibrous materials

1. Models and simulation tool

- Material models (A vs. B)
- Studied Problem
- Simulation tool : AMA

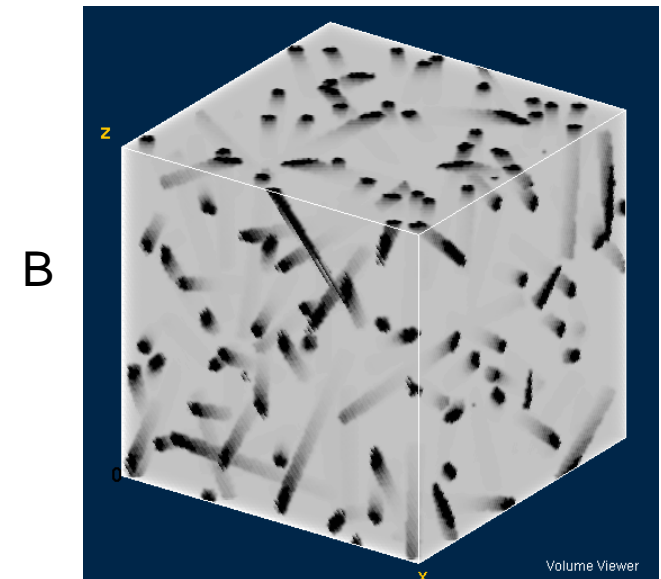
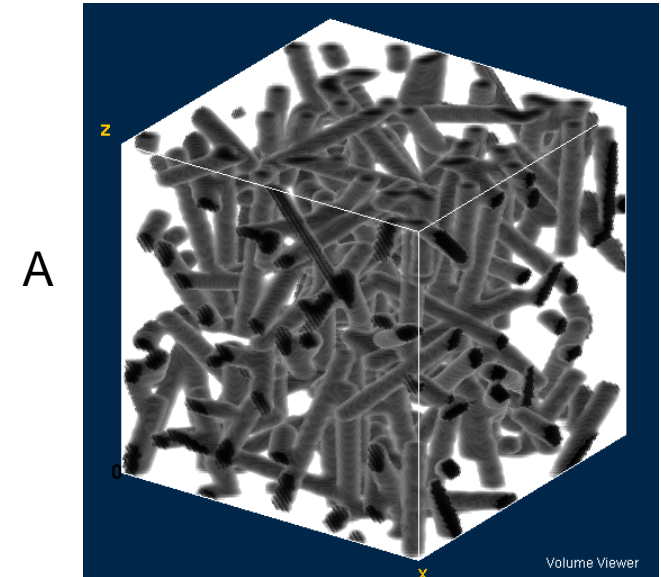
2. Simulation and analysis

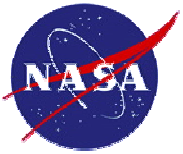
- Simulated Problem
- A vs. B: Moderate Thiele number
- A vs. B: Small Thiele number

3. Discussion

- Effective Reactive Surface Area
- Effective reactivity

4. Conclusion

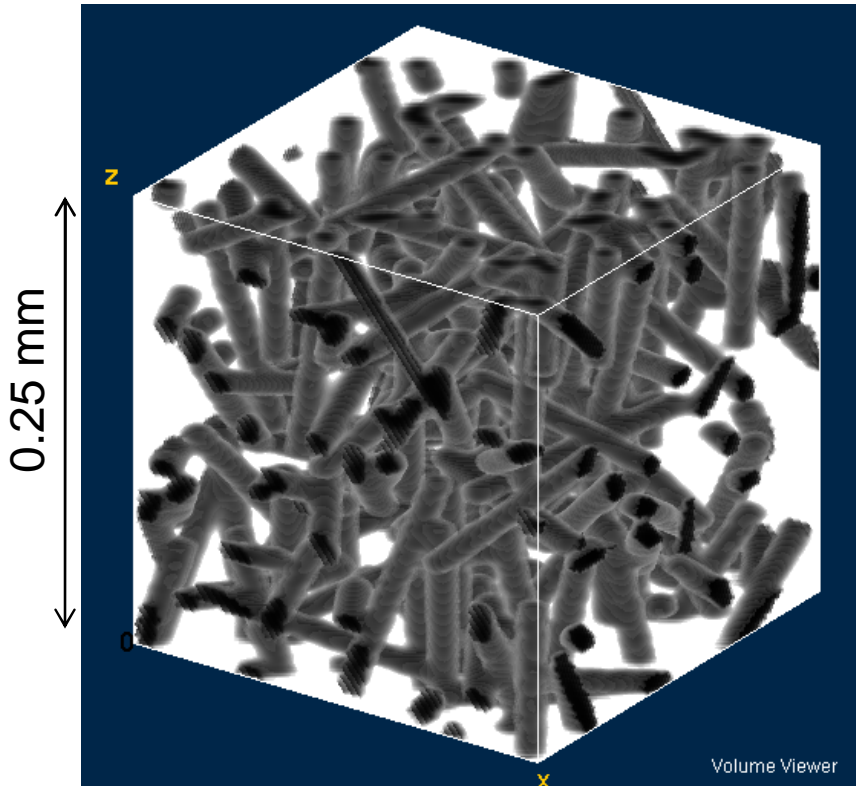




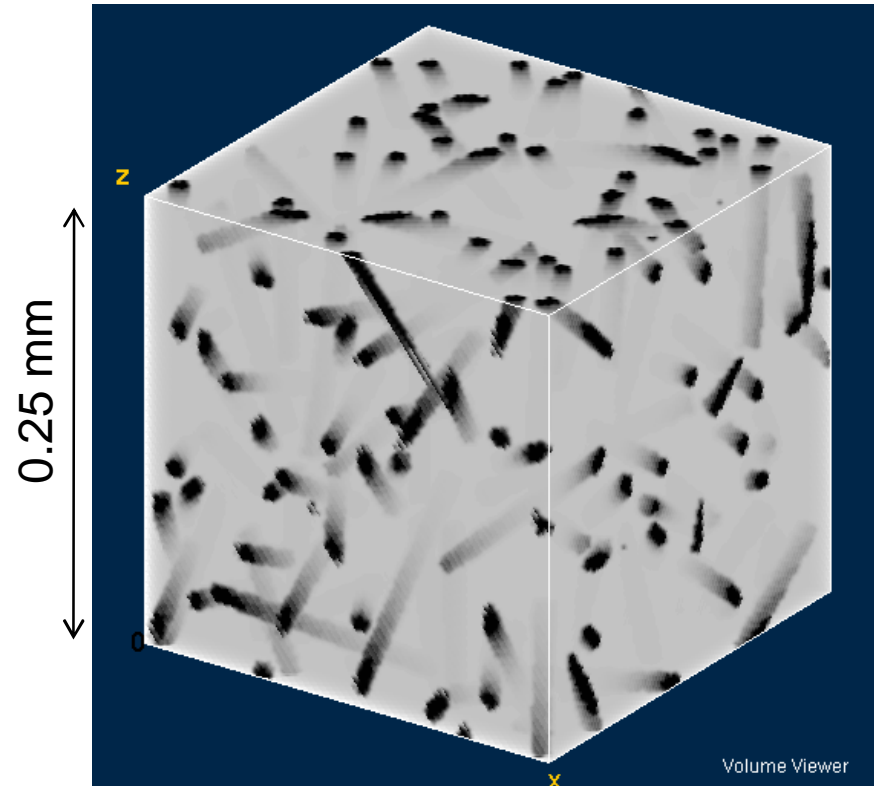
1. Models

Materials: 2 ideal low density carbon/phenolic ablators

A



B



Preform: carbon fibers, random orientations
 Fibers: diameter (10 μm), length (0.5 mm)
 Virgin mass fractions: carbon fiber (65%), Phenolic resin (35%)
 Overall density (Virgin : 280 kg/m^3 ; Pyrolyzed: 230 kg/m^3)

Similarities

Virgin mass fractions: carbon fiber (65%), Phenolic resin (35%)
 Overall density (Virgin : 280 kg/m^3 ; Pyrolyzed: 230 kg/m^3)

Dense phenolic resin surrounding the fibers: 1 μm

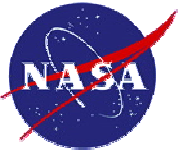
Virgin phenolic resin density: 1200 kg/m^3
 Pyrolyzed phenolic resin density: 600 kg/m^3
 Overall porosity: 0.85

Difference

Preform: carbon fibers, random orientations
 Fibers: diameter (10 μm), length (0.5 mm)
 Virgin mass fractions: carbon fiber (65%), Phenolic resin (35%)
 Overall density (Virgin : 280 kg/m^3 ; Pyrolyzed: 230 kg/m^3)

Low density pore-filling matrix

Virgin phenolic resin density: 100 kg/m^3
 Pyrolyzed phenolic resin density: 50 kg/m^3
 Overall accessible porosity: 0; **closed porosity**



1. Models and simulation tool

Ablation model: Transport, Reaction, and Local Surface Recession

- **Problem studied:** Isothermal oxidation of materials A and B in their charred form

- **Model**

Starting point : differential recession of a heterogeneous surface **S** by gasification

$$\frac{\partial S}{\partial t} + \mathbf{v} \cdot \nabla S = 0$$

Local recession velocity

$$\mathbf{v} = -J \Omega_i \mathbf{n} ; i = \{\text{fiber}, \text{matrix}\}$$

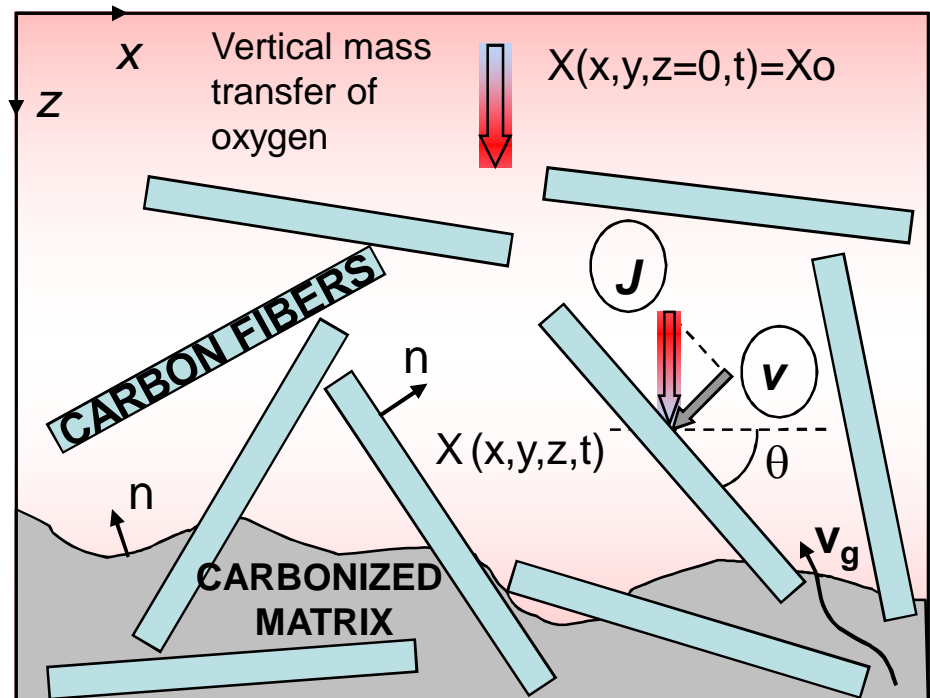
Local ablation flux per surface unit

$$J = k_i X ; i = \{\text{fiber}, \text{matrix}\}$$

Oxygen transport

$$\underbrace{\frac{\partial X}{\partial t}}_{\text{Local concentration}} + \underbrace{\nabla \cdot (-D \nabla X)}_{\text{Diffusion}} + \underbrace{\mathbf{v}_g \cdot \nabla X}_{\text{Convection (if any)}} = 0$$

Local concentration Diffusion Convection (if any)

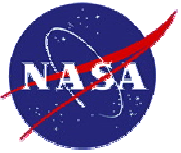


Nomenclature

X = Oxygen concentration (mol m^{-3})
 D = Diffusion coefficient ($\text{m}^2 \text{s}^{-1}$)
 k = Reactivity (m s^{-1})
 \mathbf{n} = Normal to the surface (-)
 \mathbf{v}_g = Pyrolysis gas velocity (m s^{-1})
 Ω = Solid molar volume ($\text{m}^3 \text{mol}^{-1}$)

In the following

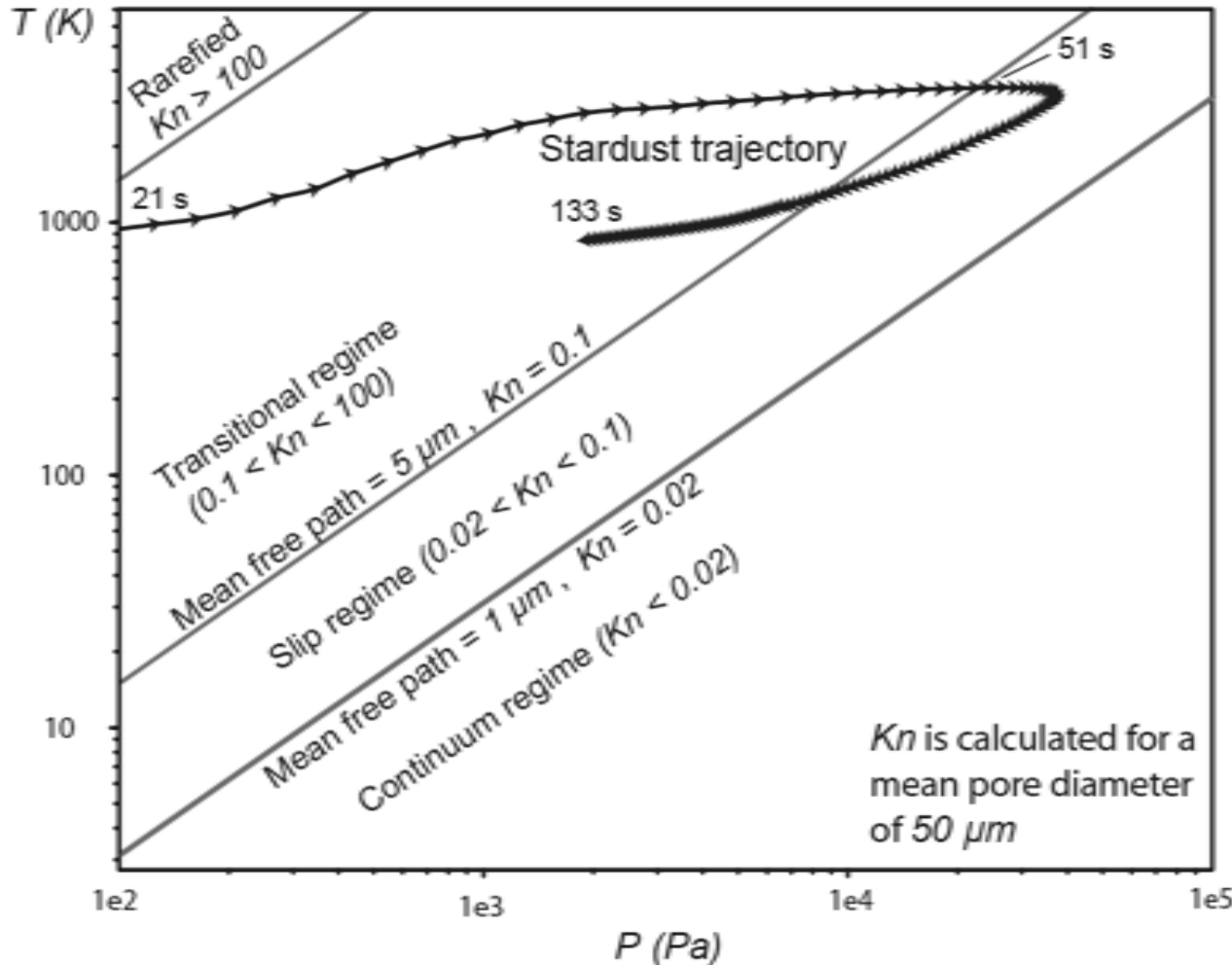
$$\mathbf{v}_g = \mathbf{0}$$



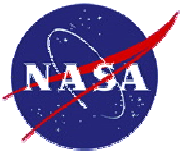
1. Models and simulation tool

Flow regime in the pores of the material [1] : from Knudsen to continuum

Just as an illustration, Knudsen number in the pores along the Stardust trajectory



[1] J. Lachaud, I. Cozmuta, N. N. Mansour. Multiscale approach to ablation modeling of phenolic impregnated carbon ablators. Journal of Spacecraft and Rockets, accepted for publication.

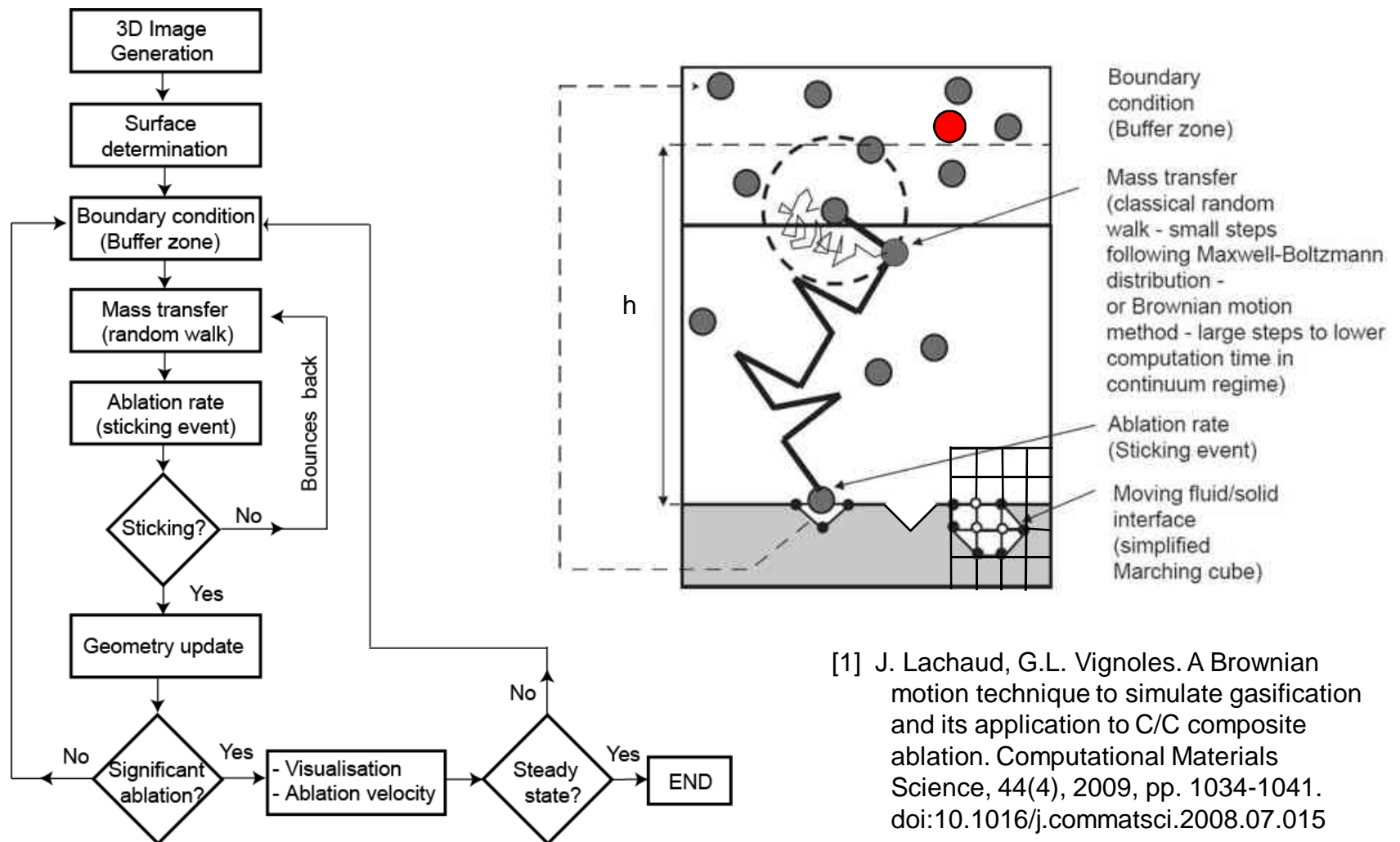


1. Models and simulation tool

Random Walk for reaction/diffusion & *Triangle Marching Cube* for surface recession

Random Walk : Knudsen & Intermediate (classical) - Continuum regime (Brownian Motion)

3D simulation tool : AMA^[1]

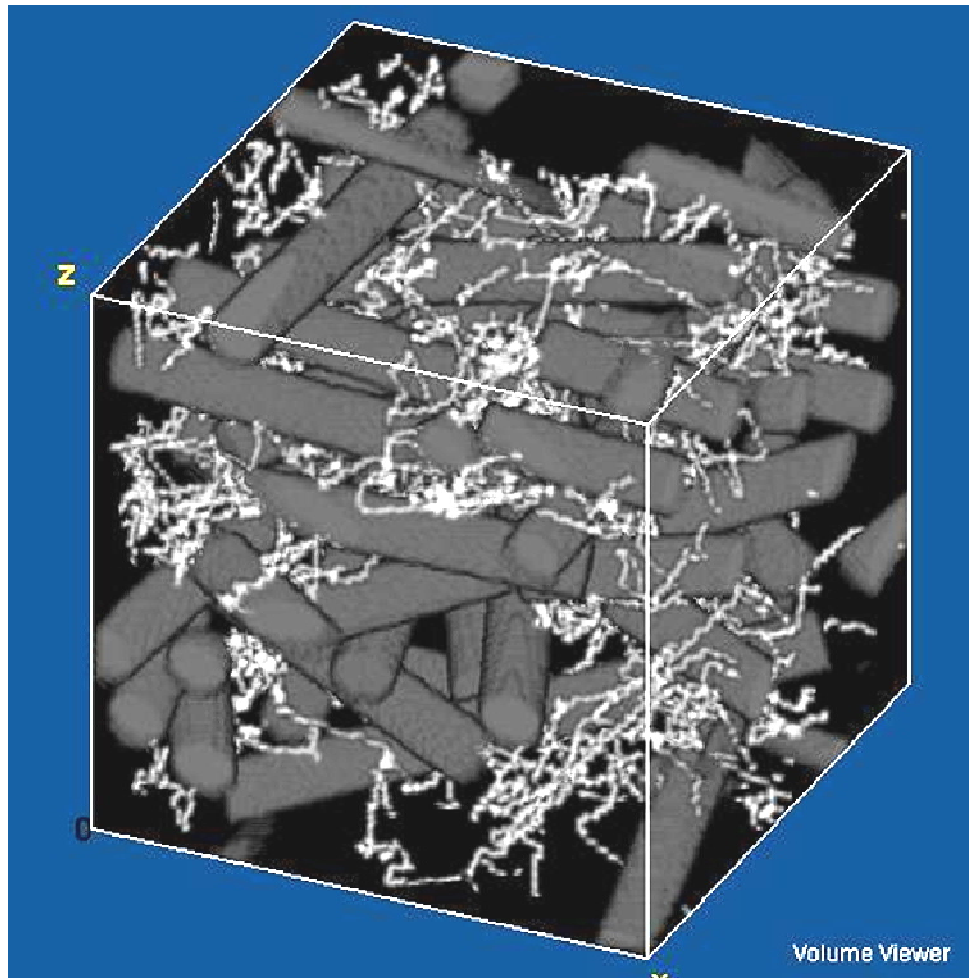




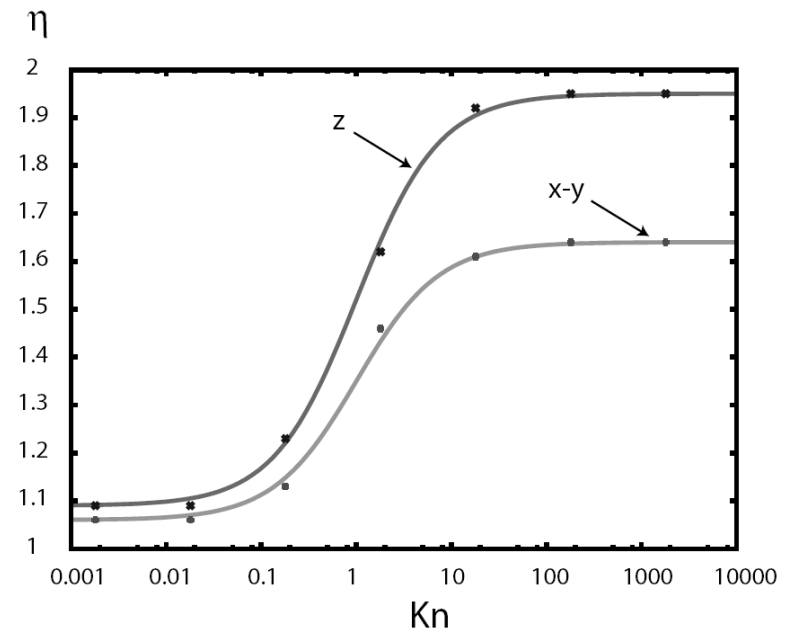
1. Models and simulation tool

Determination of the effective diffusion coefficient from first principle

Illustration : path of a walker in a periodic cell (code **AMA**).
The material in this illustration is anisotropic.

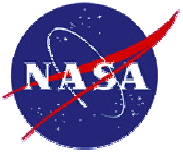


The fibrous media is tortuous. This slows the diffusion process (collisions on the walls). We can determine the tortuosity factor as a function of the mean free path of the molecules; that is, as a function of the Knudsen number.



$$D_{eff} = \frac{\varepsilon}{\eta} D_{ref}$$

← porosity (<1)
← tortuosity (>1)



. Outline

Microscopic scale simulation of the ablation of fibrous materials

1. Models and simulation tool

- Material models (A vs. B)
- Studied Problem
- Simulation tool : AMA

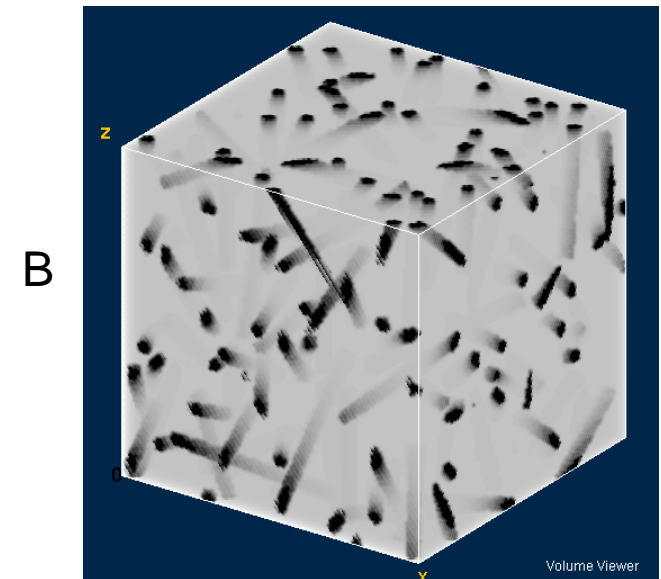
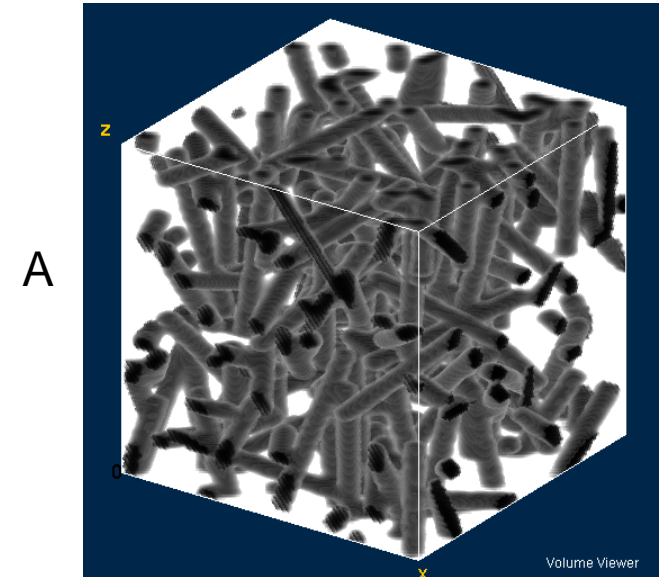
2. Simulation and analysis

- Simulated Problem
- A vs. B: Moderate Thiele number
- A vs. B: Small Thiele number

3. Discussion

- Effective Reactive Surface Area
- Effective reactivity

4. Conclusion





2. Simulation and analysis

Fiber preform : 1D steady-state analysis (diffusion time \ll ablation time)

- The concentration field is a function of the Thiele number

$$X(z) = X_0 \frac{\cosh[\Phi(z/L_s - 1)]}{\cosh \Phi}$$

Thiele number

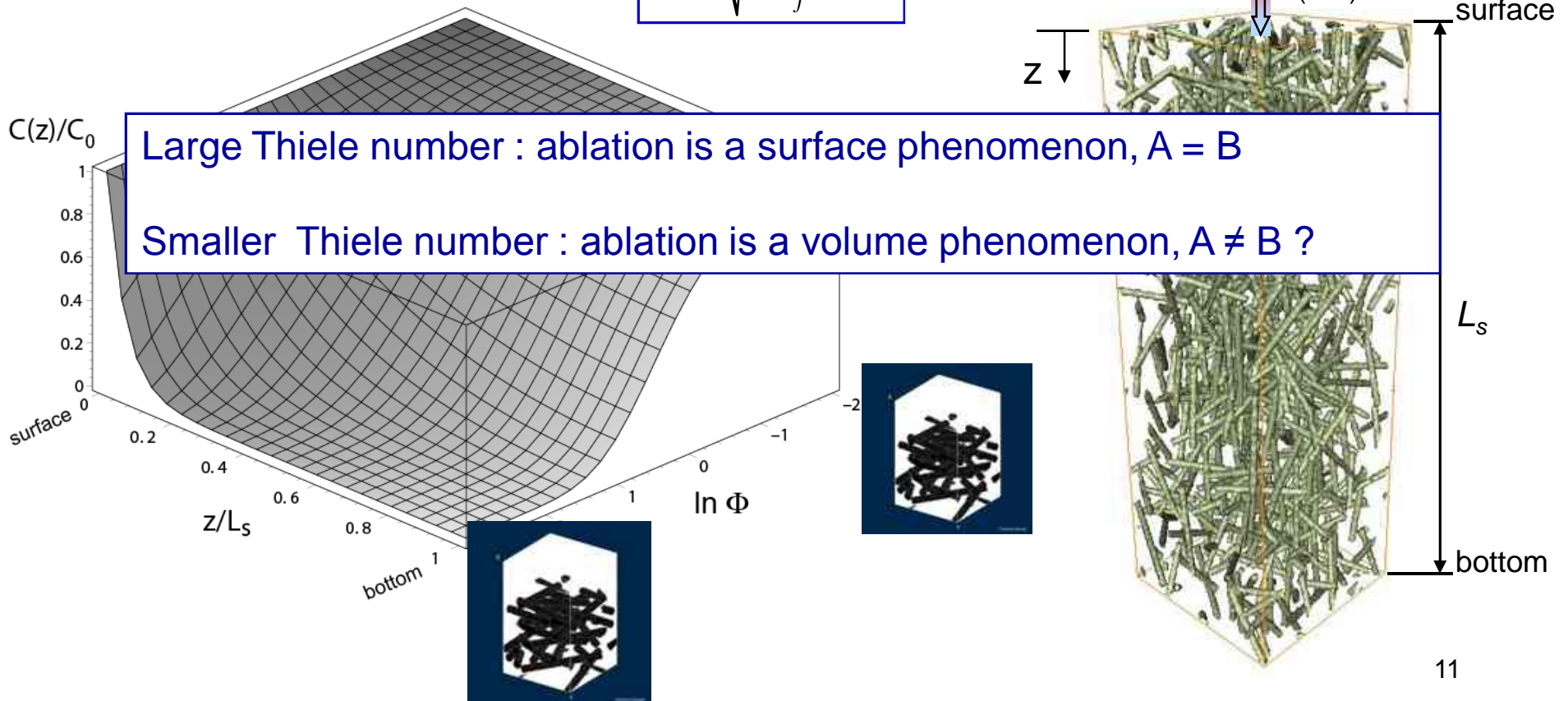
$$\Phi = \frac{L_s}{\sqrt{\frac{D_{eff}}{sk_f}}}$$

L_s : material depth (m)

D_{eff} : effective diffusivity (m^2/s)

k_f : fiber reactivity (m/s)

s : specific surface (m^2/m^3)





2. Simulation and analysis

Oxidation of B at moderate Thiele Number, $\Phi = 40$

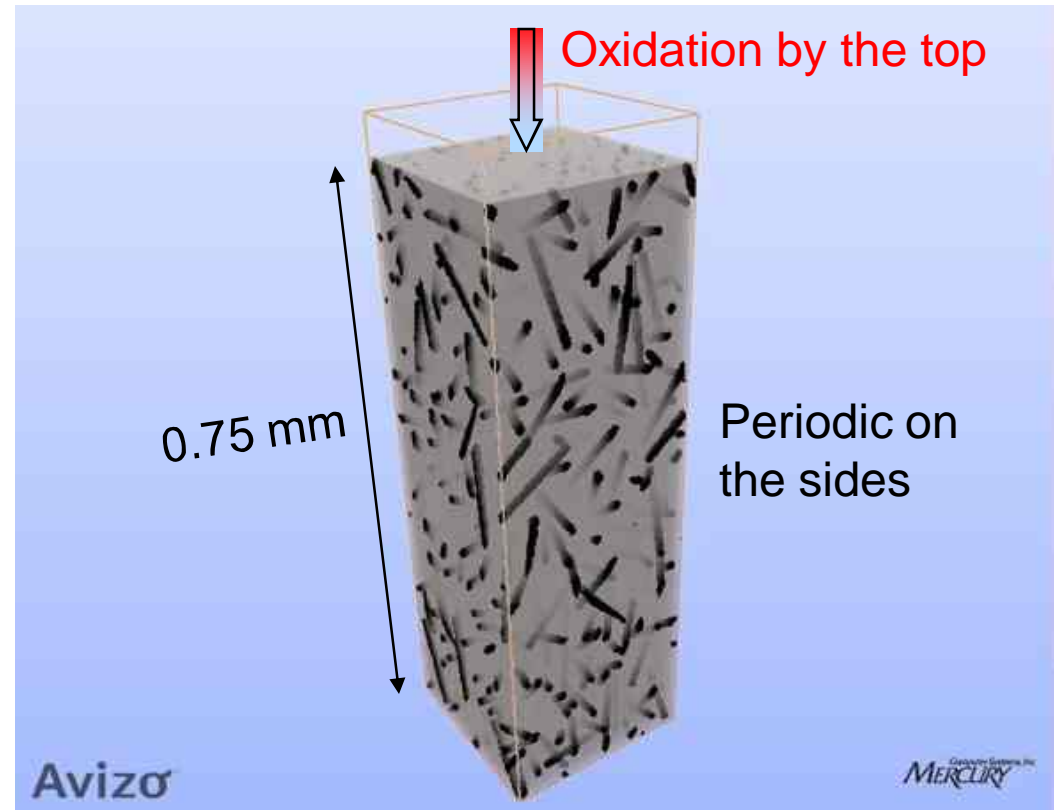
- **Hypotheses**

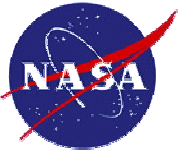
- B is fully charred
 - No pyrolysis gas blowing
 - Air
 - **$\Phi = 40$, e. g.**
 - $T = 3360$ K (isothermal)
 - $P = 0.26$ Atm
 - $\rho_f = 32 \rho_m$
 - oxidation by O_2
- $k_m = 10$ $k_f = 13.7$ m/s
[Drawin 1992, Lachaud 2007]

N.B.: oxidation by O

$k_f = 100$ m/s [Park], $\Phi > 1000$

- Diffusion/reaction DSMC simulation
 - Physical time: 1.2 s
 - Computational time : 2 days on a single core.





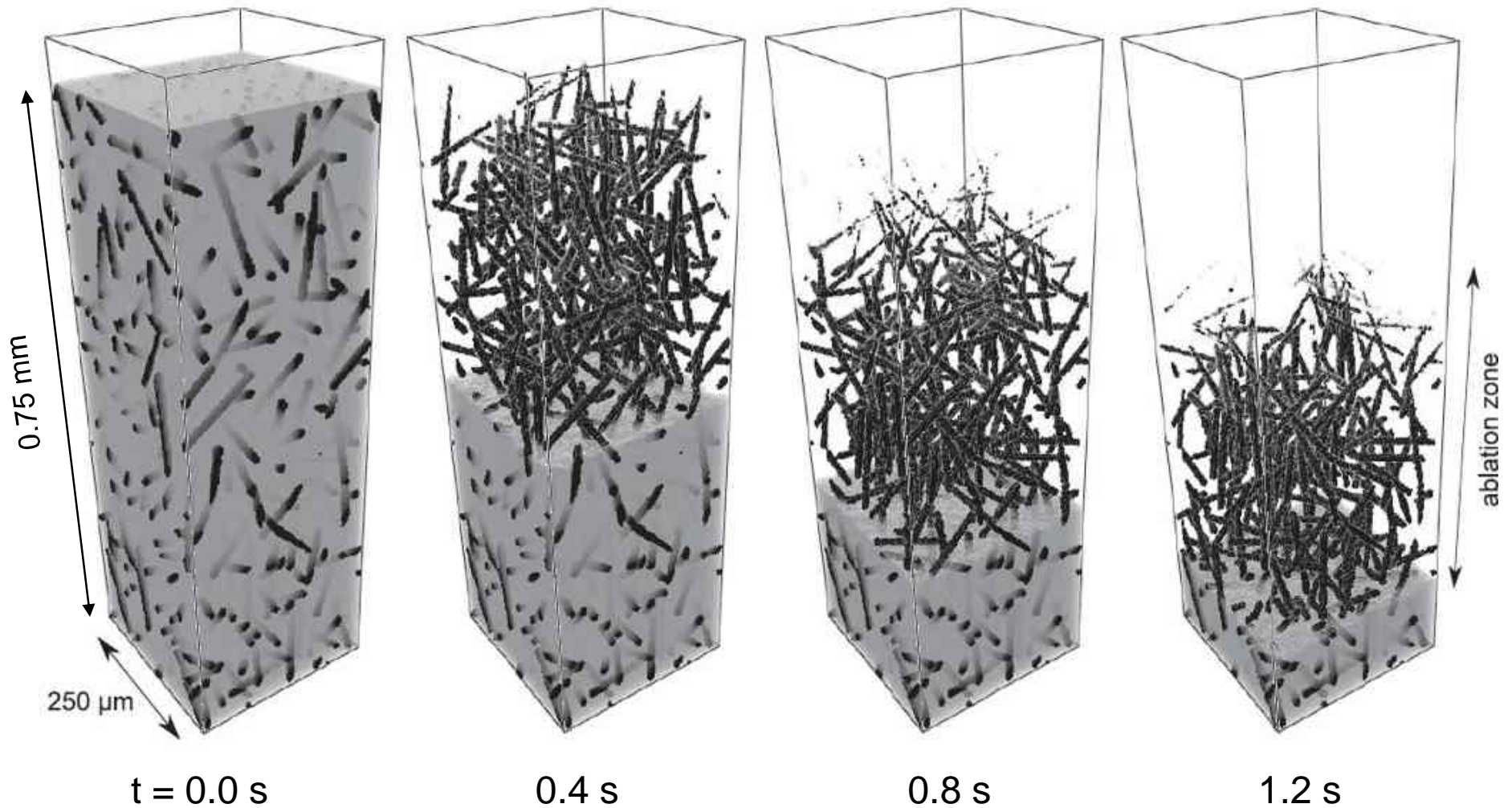
2. Simulation and analysis

Oxidation of B at moderate Thiele number ($\Phi = 40$): 3 stages

1) Matrix is removed first

2) Fiber diameter decreases

3) Overall surface recession

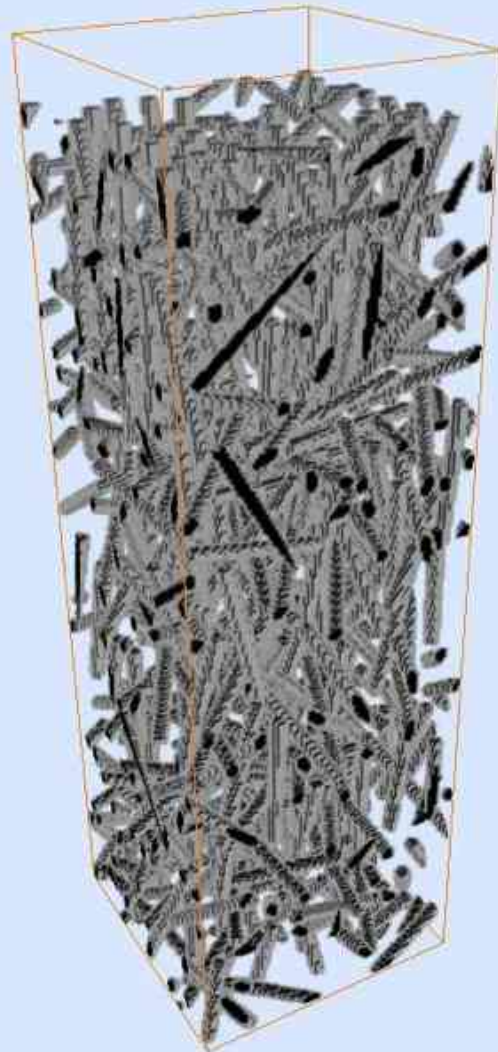




2. Simulation and analysis

Same conditions ($\Phi = 40$): Comparison of A & B

A

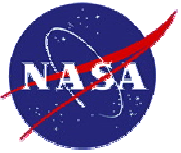


Avizo[®]

B



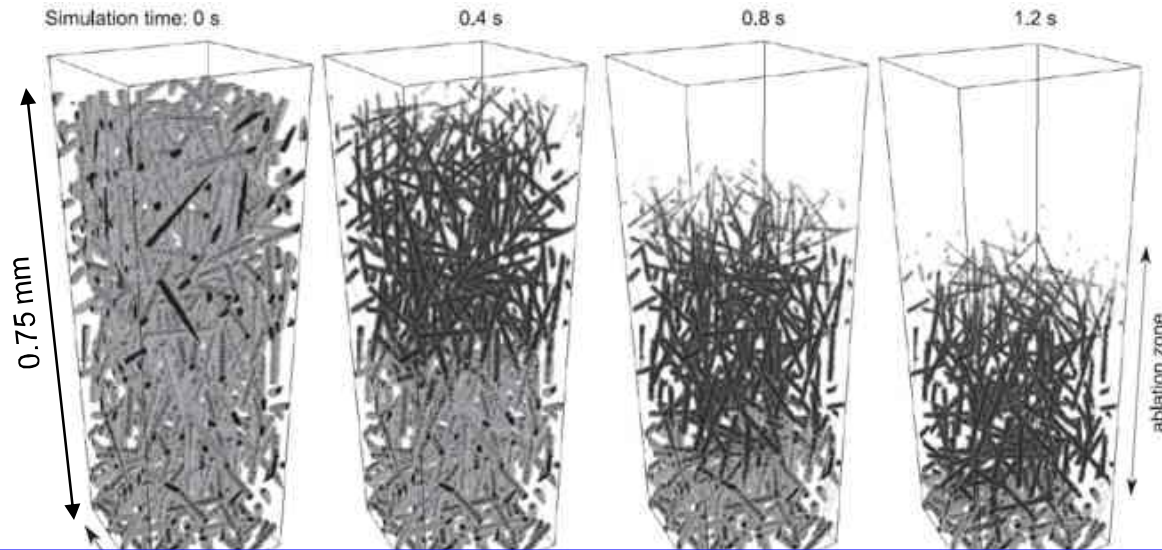
Avizo[®]



2. Simulation and analysis

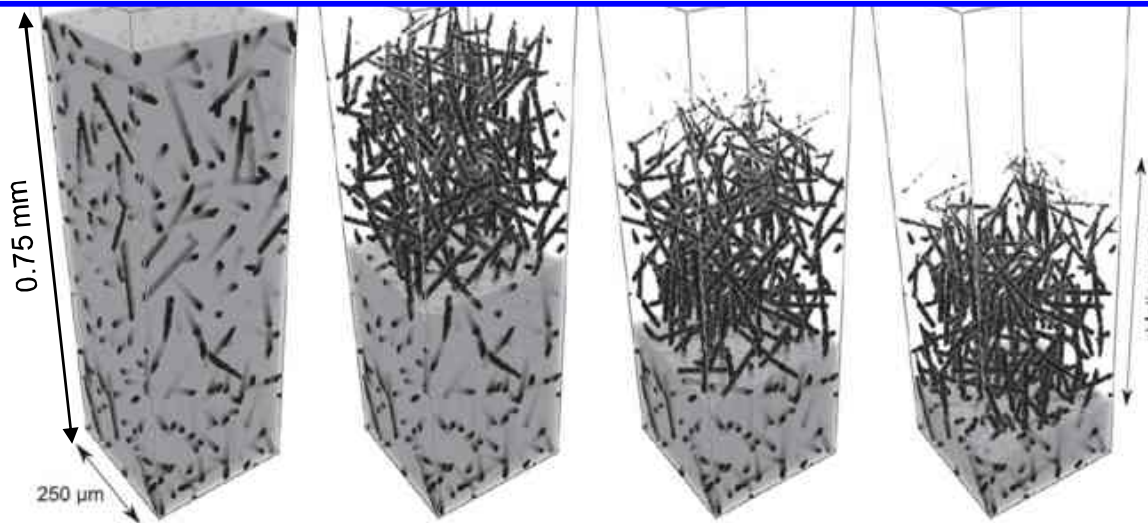
Same conditions ($\Phi = 40$): Comparison of A & B

Material A



Similar behaviors at high and moderate Thiele number
i.e, high temperatures

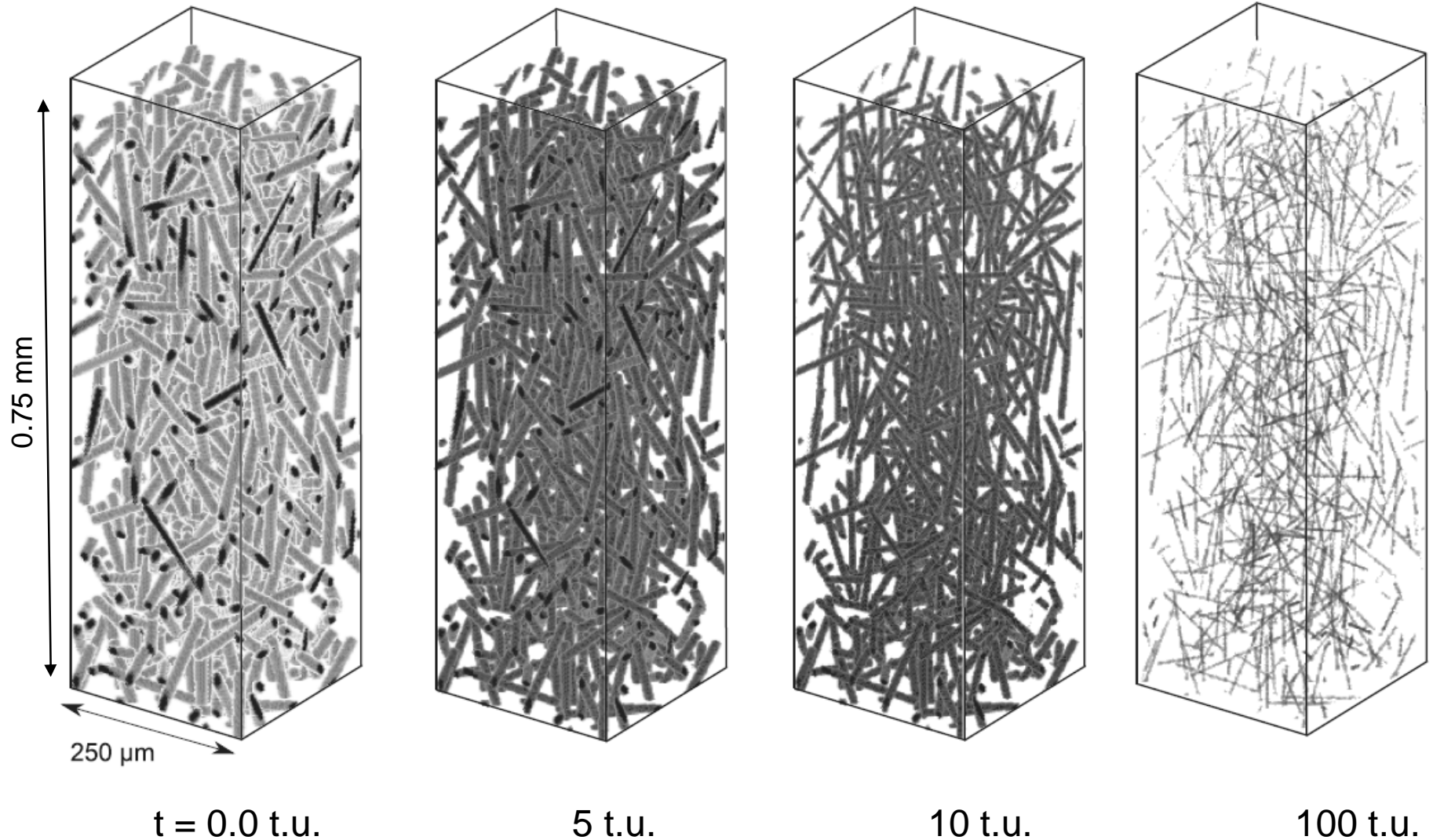
Material B





2. Simulation and analysis

Small Thiele number ($\Phi < 0.01$); Material A



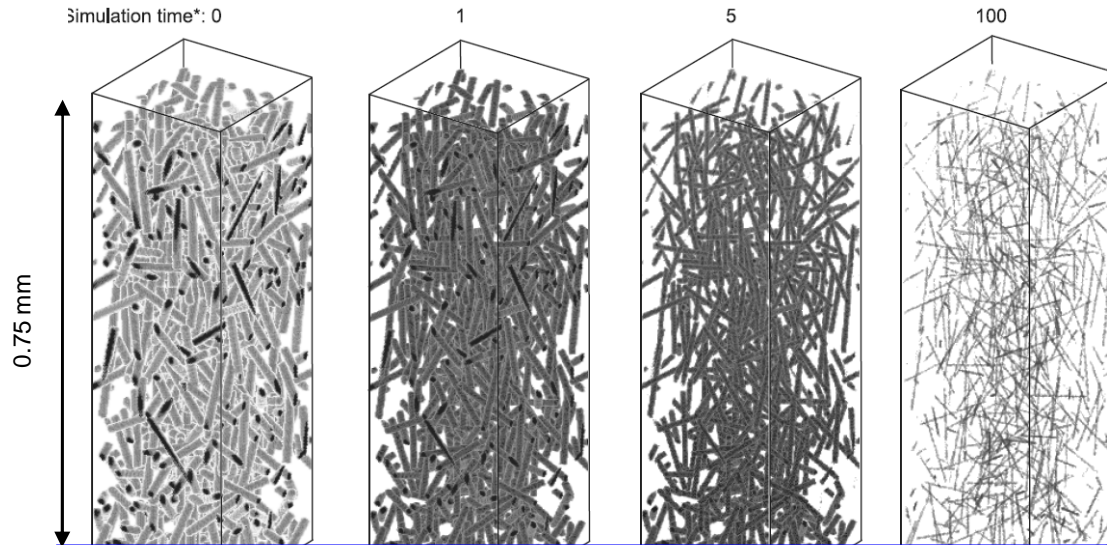
At $T=1000 \text{ K}$, 1 t.u. \approx 4 minutes, oxidation by molecular oxygen.



2. Simulation and analysis

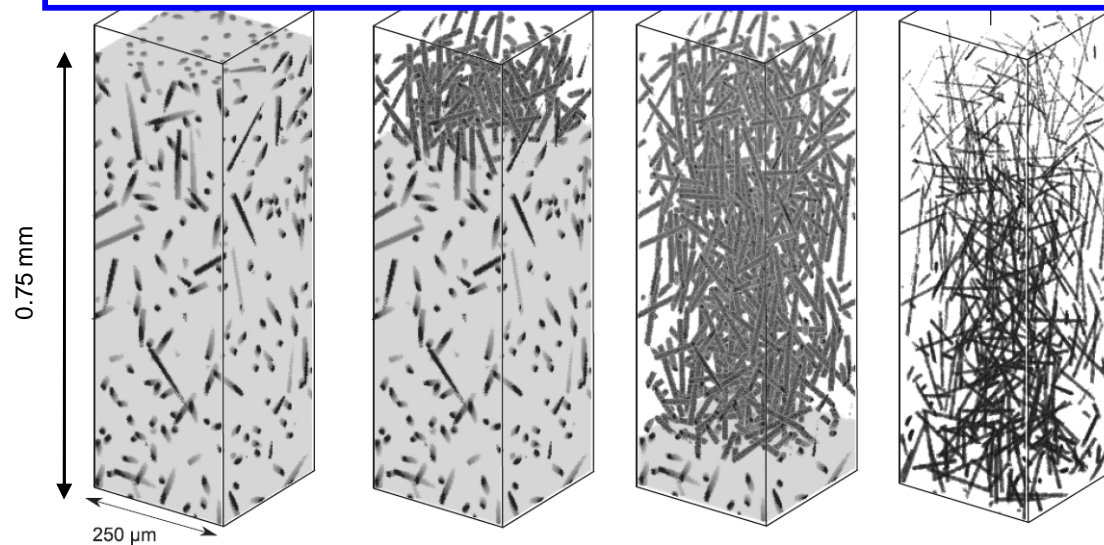
Small Thiele number ($\Phi < 0.01$): comparison of A and B

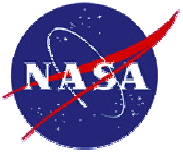
Material A



Different behaviors at small Thiele numbers
i.e., moderate temperatures

Material B





. Outline

Microscopic scale simulation of the ablation of fibrous materials

1. Models and simulation tool

- Material models (A vs. B)
- Studied Problem
- Simulation tool : AMA

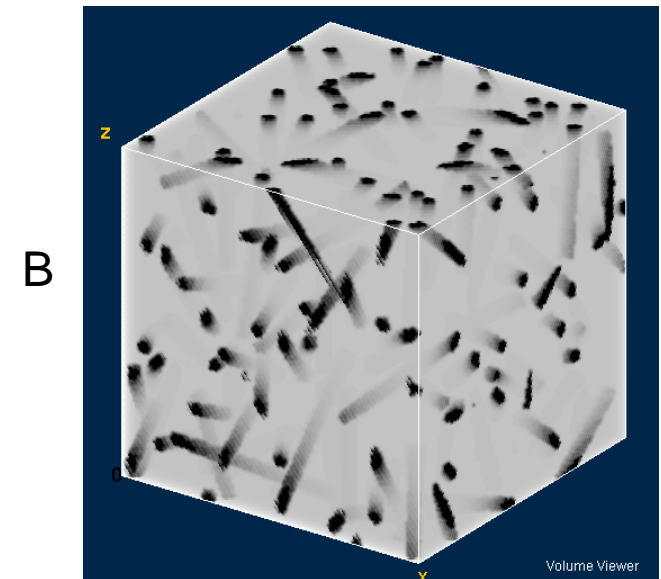
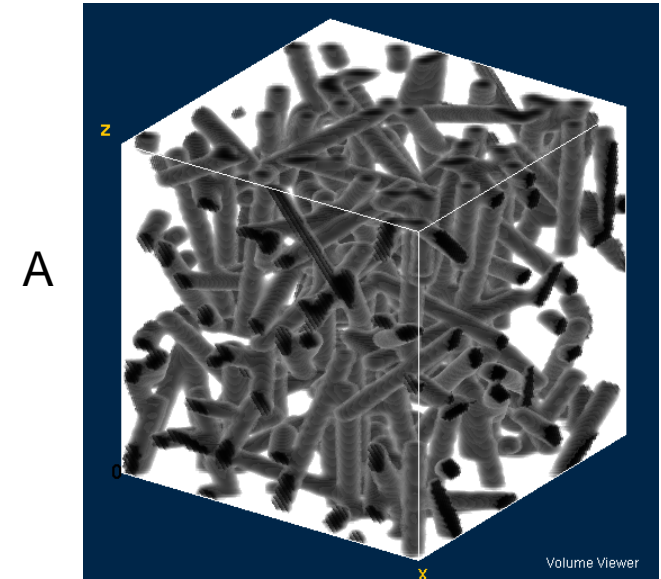
2. Simulation and analysis

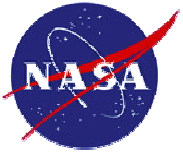
- Simulated Problem
- A vs. B: Moderate Thiele number ($\Phi=40$)
- A vs. B: Small Thiele number ($\Phi=40$)

3. Discussion

- Effective Reactive Surface Area
- Effective reactivity model

4. Conclusion





3. Discussion

Effective Reactive Surface Area (ERSA). Illustration: fiber preform [1].

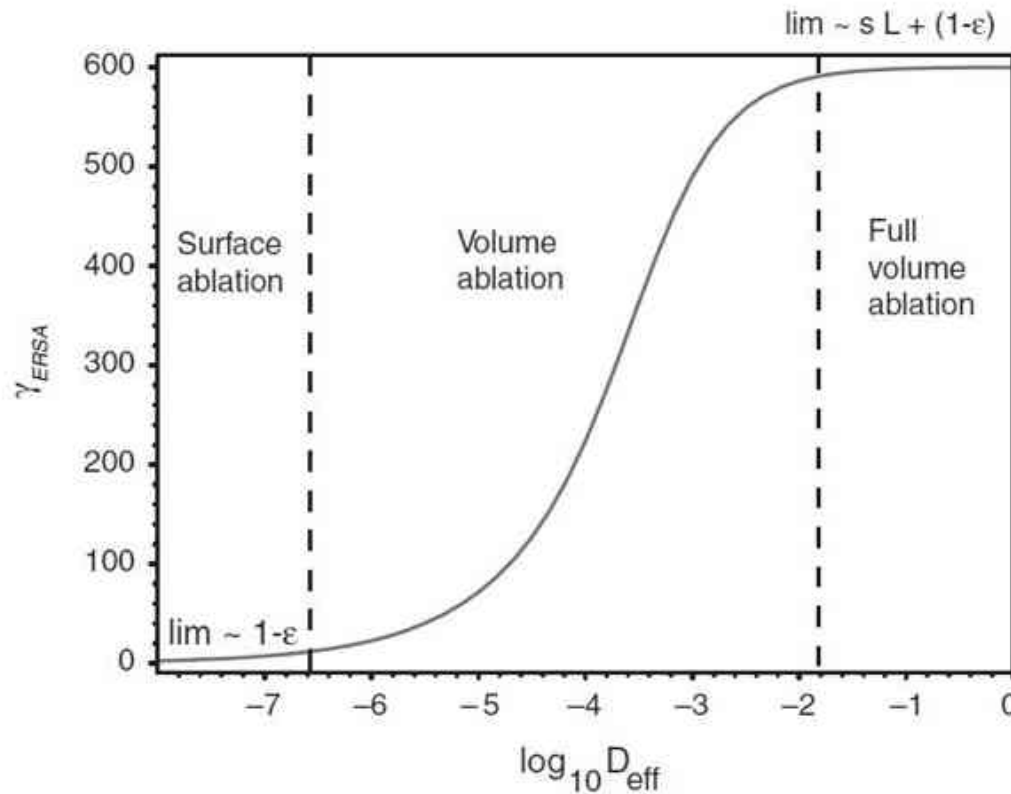
For a fiber preform, the effective reactivity is $k_{eff} = \gamma_{ERSA} k_f(T)$

$$\gamma_{ERSA} = \frac{ERSA}{GSA} = \int_{z=0}^L s_f X(z) / X_0 dz = \left[sL \frac{\tanh \phi}{\phi} + (1 - \varepsilon) \right]$$

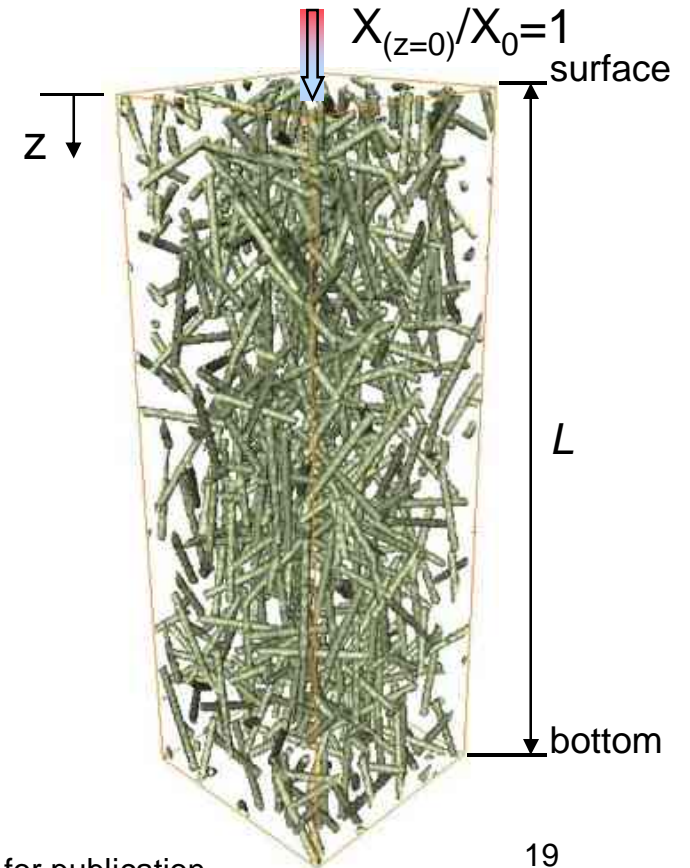
L_s : material depth (m)
 D_{eff} : effective diffusivity (m²/s)
 k_f : fiber reactivity (m/s)
 s : specific surface (m²/m³)
 GSA : geometric surface area (m²)

Thiele number

$$\Phi = \frac{L_s}{\sqrt{\frac{D_{eff}}{s k_f}}}$$



Plotted for: $k_f=1$ m/s; $L=1$ cm; $s=6 \times 10^5$ m²/m³

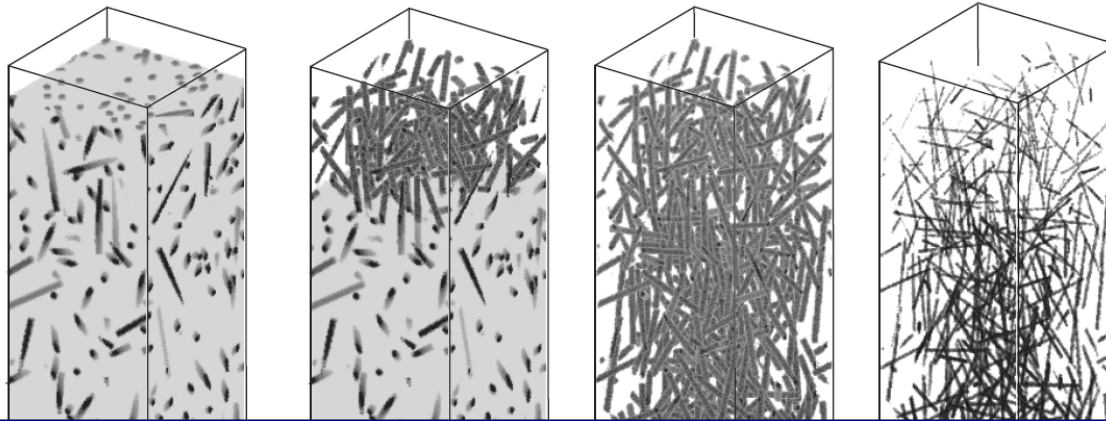


[1] J. Lachaud, I. Cozmuta, N. N. Mansour. Multiscale approach to ablation modeling of phenolic impregnated carbon ablators. Journal of Spacecraft and Rockets, accepted for publication.



3. Discussion

Effective reactivity of material B at small Thiele number ($\Phi < 0.01$)

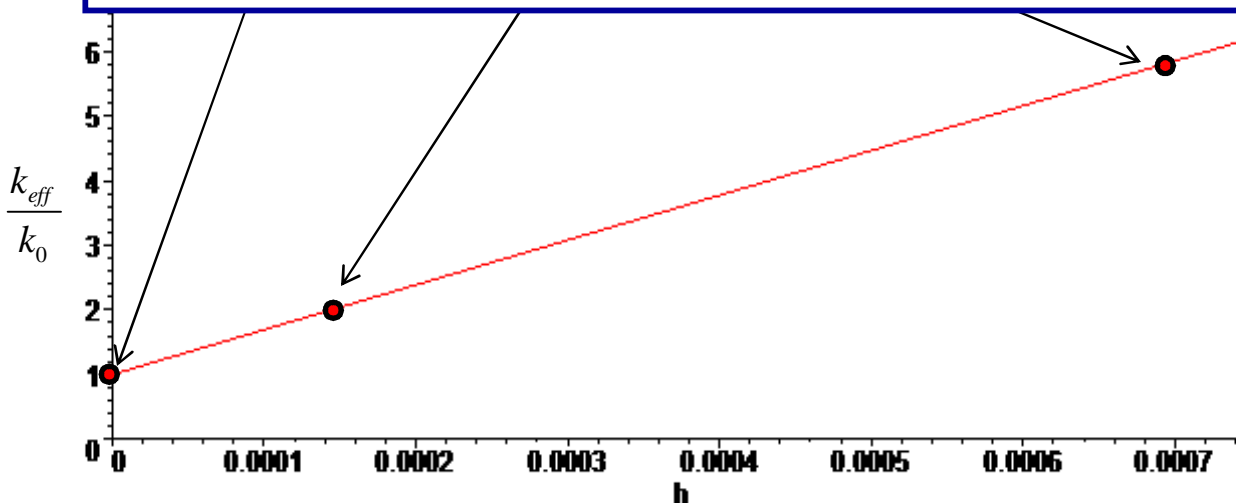


In this case, the effective reactivity can be estimated analytically under the following hypotheses:

- No temperature gradient
- No pyrolysis gas flux
- The fiber diameter reduction is small

We are currently working on the development of more elaborated models including

- Temperature gradients,
- Homogeneous finite-rate chemistry (ablation and pyrolysis gases)



$$k_{eff} = k_0 \left[1 + \frac{(\epsilon_m k_m / k_f + \epsilon_f)}{s} \right]$$

- k_0 : reactivity at $t=0$ (m/s)
- s : specific surface (m^2/m^3)
- h : matrix depth (m)
- ϵ_f : fiber volume fraction
- k_f : fiber reactivity (m/s)
- ϵ_m : matrix volume fraction
- k_m : matrix reactivity (m/s)

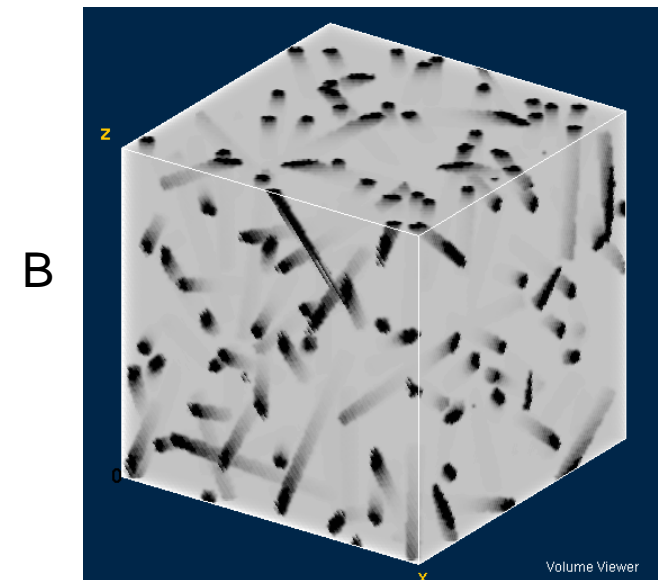
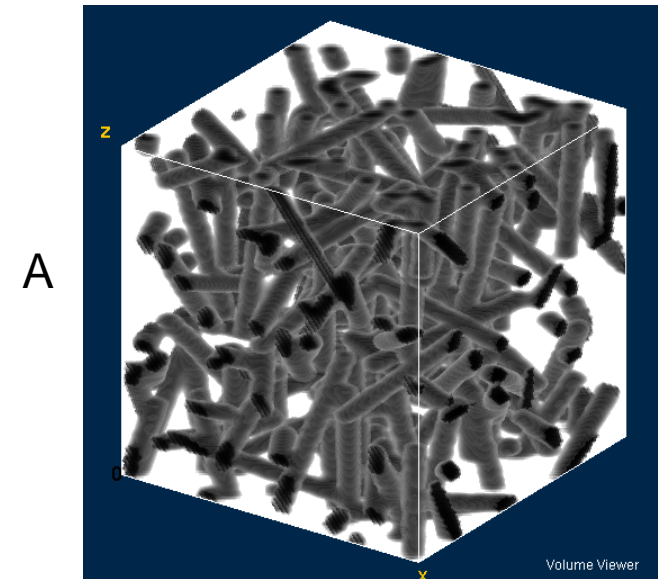


. Conclusion and perspectives

- ✓ New volume ablation model (oxidation only)
 - Large Thiele number : $A \approx B$
(usually high temperatures)
 - Smaller Thiele number : $A \neq B$
(usually moderate and low temperatures)

- ✓ Finite-rate chemistry
 - **The effective reactivity of a material is not only a function of the temperature.** It is also a function of the ERSA; that is, of:
 - the geometric surface area available
(depends on the ablation history);
 - the Thiele number;
 - the temperature gradient;
 - homogeneous reactions occurring with pyrolysis gases.

- ✓ Perspective: Application to real re-entry conditions
 - Thermal gradients
 - Pyrolysis-ablation coupling (pyrolysis gases)



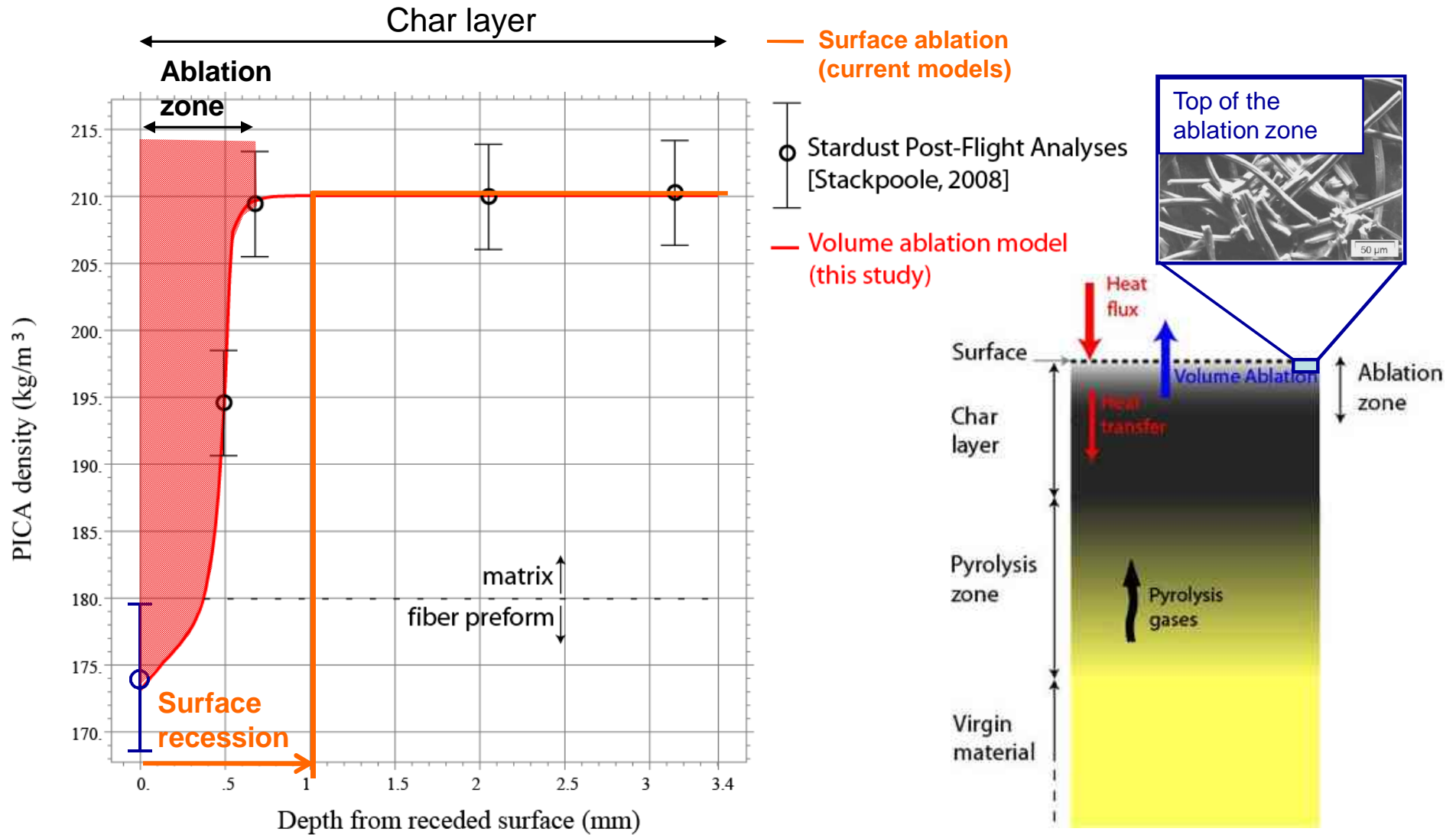


Appendix

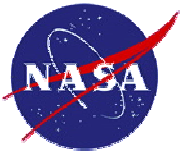


. Application to Stardust conditions

Material B : Fit of post-flight density profile [1]

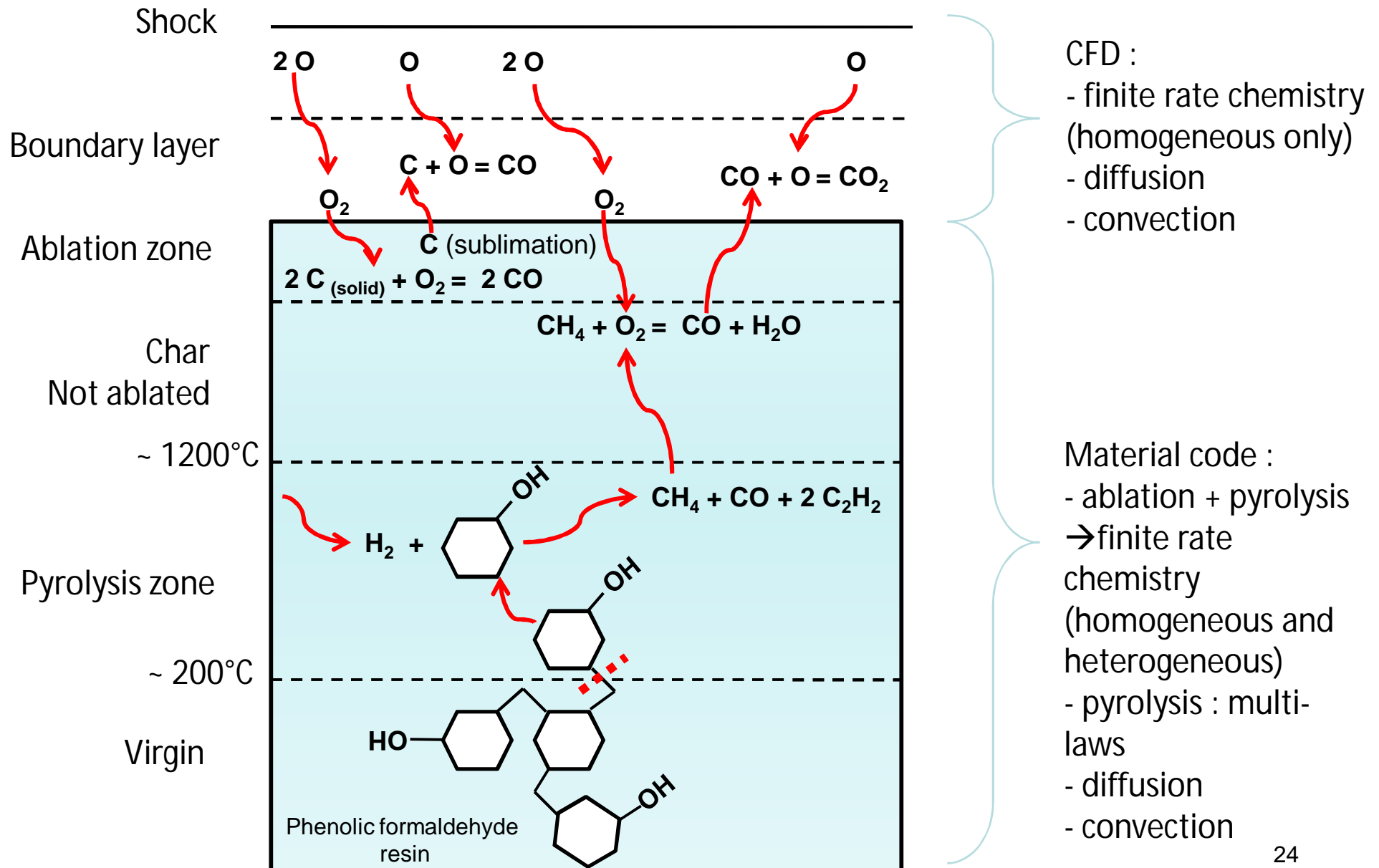


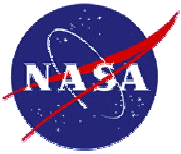
[1] J. Lachaud, I. Cozmuta, N. N. Mansour. Multiscale approach to ablation modeling of phenolic impregnated carbon ablators. Journal of Spacecraft and Rockets, accepted for publication.



. Current developments: chemistry

Pyrolysis-ablation coupling. Main problem : Finite-rate chemistry.





. Current developments: macroscopic scale model

Comparison of A & B for the end of Stardust re-entry

